Tropospheric Ozone Increases over the Southern Africa Region: Bellwether for Rapid Increases in Southern Hemisphere Pollution?

For *ACP SI2N Issue.* Revision 26 June 2014

A. M. Thompson
NASA/Goddard Space Flight Center, Code 614, Greenbelt, MD 20771 USA; also at Pennsylvania State University Dept. of Meteorology, University Park, PA 16802 USA

N. V. Balashov
Pennsylvania State University Dept. of Meteorology, University Park, PA 16802 USA

J. C. Witte
SSAI, Lanham, MD 20706 USA; also at NASA/Goddard Space Flight Center, Code 614, Greenbelt, MD 20771 USA

J. G. R. Coetzee
South African Weather Service, Pretoria, South Africa

V. Thouret
Laboratoire D'Aerologie, Obs. Du Midi-Pyrénées, Toulouse, France

F. Posny
Université de La Réunion, La Réunion, France

1

Abstract

Increases in free tropospheric (FT) ozone based on ozonesonde records from the early 1990's through 2008 over two subtropical stations, Irene (near Pretoria, South Africa) and Réunion Island (21S, 55W, ~2800 km NE of Irene in the Indian Ocean) have been reported. Over Irene a large increase in the urban-influenced boundary layer (BL, 1.5-4 km) was also observed during the 18-year period, equivalent to 30%/decade. Here we show that the Irene BL trend is at least partly due to a gradual change in the sonde launch times from early morning to the midday period. The FT ozone profiles over Irene in 1990-2007 are re-examined, filling in a 1995-1999 gap with ozone profiles taken by Measurements of Ozone by Airbus In-service Aircraft (MOZAIC) over nearby Johannesburg. A multivariate regression model that accounts for the annual ozone cycle, ENSO and possible tropopause changes was applied to monthly averaged Irene data from 4-11 km and to 1992-2011 Réunion sonde data from 4-15 km. Statistically significant trends appear predominantly in the middle and upper troposphere (UT, 4-11 km over Irene, 5-13 km over Réunion) in winter (June-August), with increases ~ 1 ppbv/yr over Irene and ~2 ppbv/yr over Réunion. These changes are equivalent to ~25% and 40-50%/decade, respectively. Both stations also display smaller positive trends in summer, with a 50%/decade ozone increase near the tropopause over Réunion in December. To explain the ozone increases, we investigated a time series of dynamical markers, e.g., potential vorticity (PV) at 330-350K. PV affects UT ozone over Irene in November-December but displays little relationship to ozone over Réunion. A more likely reason for wintertime FT ozone increases over Irene and Réunion appears to be long-range transport of growing pollution in the southern hemisphere. The ozone increases are consistent with trajectory origins of air parcels sampled by the sondes and with recent NO_x emissions trends estimated for Africa, South America, and Madagascar. For Réunion trajectories also point to sources from the eastern Indian Ocean and Asia.

1. Introduction

We are motivated to assess tropospheric ozone trends for two reasons: (1) air quality, where surface data are typically used; (2) climate perturbations, where free tropospheric ozone exercises a positive radiative forcing (Shindell et al., 2006). In the troposphere, under the influence of sunlight, ozone is formed by chemical reactions among nitrogen oxides (NO_x = NO + NO_2), carbon monoxide (CO) and volatile organic compounds (VOCs) (Brunekreef and Holgate, 2002). Ozone may also be transported vertically into the free troposphere (FT) from the ozone-rich stratosphere; this mechanism is known as stratosphere-troposphere exchange (STE; Holton et al., 1995). Trends analysis must account for natural variability in tropospheric ozone due to seasonal cycles and climate oscillations that affect both STE and sources of the ozone precursors, NO_x, CO and VOCs that originate from a range of anthropogenic and natural processes (Oltmans et al., 2012).

Most tropospheric ozone trend studies to date have focused on regional pollution in the northern hemisphere where sources are reasonably well-characterized and inter-continental transport links Asia, North America and Europe as a global phenomenon (Cooper et al., 2012; Logan et al., 2012; Parrish et al., 2012; Parrish et al., 2013). Ozone measurements from urban and rural background sites are usually used for trends studies

(Oltmans et al., 2012), with some mixture of ozone data from ozonesondes and commercial aircraft monitoring (Logan et al., 2012). Trends based on satellite ozone column estimates have been published (Beig and Singh, 2007) but the various data products available are highly uncertain (Doughty et al., 2011; Schoeberl et al., 2007; Stajner et al., 2008; Thompson et al., 2012). Satellite data for the ozone precursors NO_x (van der A et al., 2008; Lourens et al., 2011; Zien et al., 2013) and CO (Worden et al., 2009), are becoming available, but only for the period after 1995. These studies also focus on the northern hemisphere. In some cases satellite trends are based on multiple instruments with differing algorithms and sampling characteristics and thus are highly uncertain.

Data from a handful of South American megacities (Gallardo et al., 2012) and rapidly growing cities in sub-equatorial Africa represent most of our information about the southern hemisphere (SH). Trends in South American and African cities are hard to establish because a variety of ozone measurement techniques have been employed, many stations are only a few years old, and calibration checks are sometimes irregular. An exception occurs in South Africa (SA), where the Johannesburg-Pretoria (referred to below as J-P) conurbation (location of blue star in **Figure 1**) may already have attained mega-city status (Liousse et al., 2012; Liousse et al., 2014). Air quality monitoring in some parts of South Africa began in the 1970s, with adoption of high-quality, regularly calibrated instrumentation in the late 1980s and early 1990s (Rorich and Galpin, 1998). At municipal levels, dozens of stations began operating after 2005 (http://www.saaqis.org.za). To the east of J-P, at five monitoring sites over the partly rural, partly industrialized regions of the Gauteng and Mpumalanga highveld, surface ozone exhibit pronounced sensitivity to ENSO but little evidence of trends over the period 1990-2007 (Balashov et al., 2014). Oltmans et al. (2012) recently reported that the WMO/GAW (World Meteorological Organization/Global Atmospheric Watch) Cape Point station displayed a 15-20% ozone increase from 1990-2000, followed by a period of zero-to-low growth.

In order to examine possible ozone trends in the FT in the J-P region, Clain et al. (2009) used sonde data from the SHADOZ (Southern Hemisphere Additional Ozonesondes; Thompson et al., 2003; Thompson et al., 2012) station at Irene (25.9S, 28.2E). Clain et al. (2009) also studied FT ozone variability and trends at Réunion island (20.8S, 55.5E, data from 1992-2008), a SHADOZ station ~2800 km northeast of J-P (red star in **Figure 1**). A regular linear regression approach was employed to compare the 1990-1993 Irene record with SHADOZ-period (Thompson et al., 2003; Diab et al., 2004; Thompson et al., 2012) soundings that spanned 1998-2008. The trends were computed from ~1 km above the surface to 16 km for the entire sampling period, with layers 2-6 km thick. On average for Irene, only in the boundary layer (BL, in this case 2-4 km) was there a statistically significant trend, +14.4 ($\pm$4.0) %/decade. A similar analysis was performed with the Réunion sonde record, where, conversely, only above 10 km did ozone increase significantly from 1992-2008, at 12($\pm$6) %/decade.

Due to a pronounced seasonal cycle of ozone throughout the troposphere, Clain et al. (2009) also computed trends for each season: December-January-February (DJF, summer), March-April-May (MAM, fall), June-July-August (JJA, winter), September-October-November (SON, spring). There was a barely significant ozone increase in the middle troposphere (MT, 6-10 km, 12.3 [$\pm$12.2] %/decade) only in JJA. Also in JJA there was a

significant trend of 18.30 (±9.51) %/decade in 10-16 km layer. There were no other Réunion trends during individual seasons. In JJA, the Irene increase from 1990-2008 at 6-10 km was 11.4(±5.1) %/decade. Taking only the SHADOZ period, 1998-2008, that 6-10 km Irene increase more than doubled in JJA, to 28 (±14) %/decade. In the BL (2-4 km, over Irene) there was a statistically significant increase from 1998-2008, +30.5 (±12.5) %/ decade, also roughly double that over the 1990-2008 period. This ~30%/decade increase was fairly uniform throughout the year, except for a slightly higher value, +36%/decade, in MAM. Clain et al. (2009) hypothesized that the Irene and Réunion ozone growth in the lower and middle troposphere could be associated with increases in industrialization and biomass burning. However, they pointed out that the Réunion UT ozone increases occur when STE processes are most prevalent.

In this paper the Irene sondes, with additional J-P ozone profiles (1995-1999) from the MOZAIC project, and extended Réunion ozone profiles (1992-2011) are re-examined and more accurate trends are presented. The BL trends reported by Clain et al. (2009) for Irene are shown to be at least partially an artifact of changing ozonesonde launch times. Second, we merge the Irene and MOZAIC mid-tropospheric (4-11 km) profiles that are unaffected by sampling times. We use a multivariate regression model that accounts for the seasonal cycle, potential vorticity (PV) and El-Niño-South Oscillation (ENSO), to compute trends based on monthly averaged ozone mixing ratios. A late fall-early winter (May and June) trend in the MT over Irene turns out to be more than twice as large as reported by Clain et al. (2009), with more vertically diffuse regions of increase in summer (November-December). Between 4 and 5 km over Irene, ozone increases suggestive of BL change occur throughout the year, except at the local biomass burning season (SON).

We also calculate ozone trends over Réunion. In that case, we find a winter (July-August) trend from 1992-2011 that is much larger than over Irene, +40-50%/decade, above 8 km. Due to the strength of UT ozone increases over Irene and Réunion, we look for evidence of dynamical changes, using potential vorticity as a proxy for stratospheric influence. Similarly, assuming that growth in ozone precursors like NO_x and VOCs might account for the distinct ozone increases in May-August, standard emissions data bases are consulted. **Section 2** describes data sources and analytical methods. **Section 3** presents results and discussion. **Section 4** is a summary.

2. Data and Methods of Analysis.

2.1 Ozonesonde Measurements at Irene and Réunion Island

The measurements at Irene are made with Vaisala RS-80 radiosondes (prior to 2002) and RS92 radiosondes (from 2002 to 2008) coupled to Science Pump Corporation electrochemical concentration cell ozonesondes (Thompson et al., 2003; Diab et al., 1996; Thompson et al., 1996). A 1% buffered KI solution is used; this gives a measurement of tropospheric ozone with 5% accuracy and precision (Johnson et al., 2002; Smit et al., 2007; Smit and ASOPOS, 2011; Thompson et al., 2007). Comparisons of total column ozone from integration of the Irene sonde data from 1998-2008 (less a gap from 2000-2004) with the co-located Dobson No. 89 spectrophotometer, and with Earth-Probe/TOMS (Total Ozone Mapping Spectrometer, 1999-2004) and OMI (Ozone Monitoring Instrument, 2005-2008), are within 1%. This implies that total ozone from the Irene sondes is one of the most

accurate records in SHADOZ (see <http://croc.gsfc.nasa.gov/shadoz>; Thompson et al., 2007; Thompson et al., 2012).

Figure 2 presents a seasonal climatology of the annual cycle of FT ozone over Irene (**Figure 2a,b**) and Réunion (**Figure 2c,d**) based on monthly averages for each site. The earlier Irene record, for the years 1990-1999, as in **Figure 2a**, is based on the 1990-1993 sondes augmented by the MOZAIC record for 4-11 km for the years 1995-1999; from 1995 until late 1998 there were no sonde launches over Irene. The second Irene climatology (**Figure 2b**) is based on SHADOZ soundings for 2000-2007 with about a year of data from September 2012 through October 2013. The most recent sondes followed a 4-plus year hiatus in Irene launches that started in early 2008. The structure of the two periods depicted in **Figure 2** appears somewhat different in several time and altitude zones. One is within the TTL (tropopause transition layer), that is ~13-15 km for Irene, during June through December. Second, in the period of active southern African biomass fires (August-November), from ~4 km to 10 km, ozone appears slightly lower or unchanged in the second period (**Figure 2b**) compared with the 1990s (**Figure 2a**). Conversely, from April through July or August, ozone below 11 km appears to have increased.

Réunion Island ozonesondes have been launched since 1992 at St. Denis airport (~10masl) (Baldy et al., 1996; Baray et al., 1998; Randriambelo et al., 1999; Baray et al., 2006) using SPC and ENSCI (now Droplet Measurement Technology [DMT]) ECC ozonesondes with a 1% buffered KI solution from 1992 to 1998 and a 0.5% buffered KI solution after 1998. Several types of radiosondes have been used: Vaisala RS-80 radiosondes (prior to September 2007), Modem M2K2 sondes (from September 2007 to March 2013) and Modem M10 (from March 2013 to now). The mean 4-15 km ozone mixing ratio appears in **Figure 3a** with the frequency of sonde launches in **Figure 3b.** The most recent evaluation of total ozone over Réunion as measured by the sondes averages within 2% of the satellite reading (Thompson et al., 2012) and the ground-based Système D'Analyse par Observations Zénithales (SAOZ) instrument. Climatologies for 1992-2001 and 2002-2011, based on the soundings depicted in **Figure 3b,** are illustrated in **Figures 2c** and **2d**. Winter ozone increases above 4 km over Réunion are pronounced in JJA; in the MT there appear to be increases in October and November as well.

The 1990-1993 Irene ozonesondes were launched at 0730-0830 local time (UTC + 2hr; **Figure 4a**). When operations were resumed for SHADOZ in late 1998, launches were conducted ~0930 local. After 2002, launches fluctuated from ~1130 to 1530 local to accommodate overpasses of ozone instruments on ENVISAT (SCanning Imaging Absorption spectroMeter for Atmospheric CHartographY, SCIAMACHY) and the Aura satellite (four ozone sensors). The typical mean 1.5-4-km ozone mixing ratio in 1990-1993 (e.g. Figure 5 in Thompson et al., 1996) was ~25 ppbv in summer (DJF) with a spring maximum (SON) at 70 ppbv (**Figure 4b**). By 2006 the DJF (low ozone season) near-surface ozone had drifted upward to 30 ppbv and the mean 1.5-4 km ozone exceeded 80 ppbv, levels not seen in the early 1990s. Thus, the Clain et al. (2009) trend for SON based on comparing the 2-4 km tropospheric ozone column amounts between 1990 and 2008, was a statistically significant increase of +1.17 ($\pm$ 0.49) DU/decade, equivalent to 15 ($\pm$ 6.2)%/ decade. During the SHADOZ period only, 1998-2008, with the sampling times drifting later into the day, the 2-4-km-layer ozone increase for SON calculated by Clain et al. (2009) was 2.4 ($\pm$ 1.5)

DU/decade or 28.9 (±18)%/decade.

Figure 4c shows that at Irene, ~1.5 km above sea level, the correlation between ozone mixing ratio and launch time is 0.6. The correlation drops sharply above 2 km but the correlation coefficient is still > 0.2 at 2 km. Only above 4 km does the ozone-launch time correlation decrease to <0.08. Consequently, trends from sondes based on data below 4 km are assumed to be unreliable. The apparent BL trend noted by Clain et al. (2009) might be observed because midday surface ozone in the Pretoria region (http://www.saaqis.org.za) is typically 3-4 times greater than at 0700 local due to the daily photochemical ozone cycle.

2.2 MOZAIC Data Selection

MOZAIC sampling with Johannesburg landing and takeoffs began in 1995 and ended in 2009; coverage after 2001 was less regular than in the 1990s, with some years skipped altogether. The general coherence of the MOZAIC Johannesburg and Irene ozone profiles up to ~12 km (200 hPa) has been described by Diab et al. (2003) and Clain et al. (2009). More detailed sonde-MOZAIC comparisons reported by Thouret et al. (1998) found that above 400 hPa, ozonesondes exhibit higher values than the Airbus instrument. The middle and UT air sampled by the aircraft at beginning of descent and end of ascent is north of Johannesburg, largely over Zambia and Zimbabwe. Those profile segments correspond to a lower background ozone amount than over Irene where most sondes travel over the SA highveld and often encounter higher ozone from mid-latitude air and STE events (see, for example, a comparison of soundings over Lusaka [Zambia] and Irene in September 2000; Thompson et al., 2002). Below 400 hPa, agreement between MOZAIC and Irene profiles is usually within 5%, the stated uncertainty of the sonde instrument (Thouret et al., 1998). Because ozonesonde data over Irene is missing for most of the 1994-1998 period, we want to fill the gap with 4-11 km measurements from the MOZAIC record. A check for instrument bias between the Irene and MOZAIC ozone profiles appears in **Figure 5** where the difference between the Irene ozonesonde climatology combined from 1990-1993 and 1999-2007 and mean ozone from MOZAIC in 1995-1999 is presented. Hatched areas represent times and regions where, within the standard deviation for each data set (sonde and MOZAIC) the means of the two climatologies do not overlap. As expected, most of the statistically significant differences are above 9 km. The greatest differences appear in autumn (MAM), not in winter, which turns out to show the largest ozone trends (**Section 3**). Accordingly, for our analysis, the 1995-1999 MOZAIC and Irene data are merged into a single time-series (**Figure 6**). Furthermore, because Thouret et al. (1998) found no difference in morning or evening MOZAIC profiles in the FT, all the available data are included in the monthly averages in **Figure 6.**

2.3 Dynamical Factors and Trends Analysis

A number of studies point to significant dynamical influences that need to be taken into account in a trends analysis of FT and TTL tropical ozone. For example, examination of tropical tropospheric ozone variability with indicators of ENSO (El-Niño Southern Oscillation) based on satellite and sonde data (Chandra et al., 1998; Thompson and Hudson, 1999; Fujiwara et al., 1999; Thompson et al., 2001; Logan et al., 2008) reveals a positive (increased) ozone response in some regions, negative in others. Time-series analyses of SHADOZ ozone profiles in the troposphere and lower-stratosphere (LS) have been carried

out by Lee et al. (2010), Randel and Thompson (2011), Oman et al. (2011). At the sites equatorward of 15S/N, the ENSO signal exhibits varying characteristics, with stations responding with positive ozone and temperature anomalies (for example, Kuala Lumpur and San Cristobal), negative at others (Natal and Nairobi in Lee et al., 2010) and with distinct time-lags (Randel and Thompson, 2011). Using a different diagnostic, gravity wave frequency (GWF) as inferred from ozone and potential temperature laminae within the ozone and radiosonde profiles, Thompson et al. (2011) found that ENSO signatures during the SHADOZ record were most pronounced in the TTL and less so in the MT. Over subtropical Irene and Réunion, GWF is 2-3 times lower than over Kuala Lumpur, Watukosek and San Cristóbal (Thompson et al., 2011).

STE is known to affect tropospheric ozone at Irene especially during the spring. STE processes may occur slowly as through the Brewer-Dobson circulation (Holton et al., 1995). Alternatively, meteorological phenomena such as intense cumulus convection, tropopause folding associated with upper level troughs, and cutoff lows are the examples of faster STE mechanisms (Rao et al., 2003). It is standard practice to use potential vorticity (PV) as a dynamical tracer of stratospheric air intrusions into FT, as for example, in tropopause folds, where UT subsidence transports ozone-rich LS air into the mid-troposphere (Keyser and Shapiro, 1986; Beekmann et al., 1994; Rao et al., 2003). Consequently, any diabatic heating processes can alter PV values without affecting ozone.

Accordingly, FT ozone, at both Irene and Réunion is analyzed with a multivariate regression model that includes factors of the semi- and annual cycles, trend, ENSO, and PV variability. Such statistical regression models are common in the atmospheric sciences (Randel and Cobb, 1994; Ziemke et al., 1997). The model can be presented as:

$$\hat{T}(t) = \alpha + \beta \cdot t + \gamma \cdot ENSO(t) + \delta \cdot PV(t) + \epsilon(t), \quad (1)$$

where α is seasonal cycle fit, β is trend coefficient, t is time in months, γ is regression coefficient for the time series $ENSO(t)$, δ is regression coefficient for the $PV(t)$ time series and finally $\epsilon(t)$ is the residual that is calculated by subtracting the modeled time series $\hat{T}(t)$ from the actual ozone time series $T(t)$. For ENSO the Southern Oscillation Index (SOI; http://www.esrl.noaa.gov/psd/data/correlation/soi.data) is used as a proxy. Monthly PV averages are calculated from the ECMWF 330K PV fields over Irene (box bounded by 25.5º-32.2º S and 24.8º-31.5º E) and from the ECMWF 350K PV data over Réunion (box within 18º-25º S and 49.5º-65.25º E) (Dee et al., 2011). Note that including a PV term in Eq. (1) should partially account for any influence of a changing tropopause height (Seidel et al., 2008; Sivakumar et al., 2011). The error for each coefficient is 2 standard deviations (SD) and is estimated using a moving block bootstrap technique in order to account for auto-correlation in the ozone time series (Wilks, 1997). The model is applied to monthly mean ozone every 100 meters from 4-11 km for Irene (**Figure 7)** and over 4-15 km for Réunion (**Figure 8**). We note that the Quasi-biennial Oscillation (QBO) also affects tropical ozone (e.g., Witte et al., 2008; Thompson et al., 2011). Adding a term for the QBO in the regression model, Eq. (1), made no difference in the results, presumably because the ozone trends are mostly below 13 km, where QBO impacts are small (Lee et al., 2010).

3. Results and Discussion

3.1 Free Tropospheric Trends at Irene and Réunion

Figures 7 and 8 display ozone mixing ratio trends (in %/decade) for Irene and Réunion, respectively, based on the 100-m monthly mean ozone averages. Hatched areas, that appear only with positive trends, denote 2 SD statistical significance. At both of these stations ozone increases are most pronounced in the middle and UT, between 4 km and 11 km (Irene, **Figure 7**) and between 5 km and 13 km (Réunion, **Figure 8**) in winter. Ozone increases begin earlier in the year (April, May, June, late autumn) between 4 km and 6 km over Irene than over Réunion. In addition, in the lower free troposphere (LFT, below 5 km), statistically significant Irene ozone increases occur intermittently after June, into December (**Figure 7**). It is possible that surface ozone changes over the urbanizing J-P region play a role in the LFT change. Note that although **Figure 4** suggests that the Irene data at 5 km are free of sampling artifacts, some contamination in the 4-5 km trends (**Figure 7**) might be present.

At Réunion, there is a UT summer increase (**Figure 8,** December, January, 9-15 km) that bears some similarity to an Irene increase at 10-11 km in November and December (**Figure 7**), but the magnitude of the Réunion ozone change is slightly greater than the Irene signal. In particular, 13-15 km layer over Réunion shows a significant ozone enhancement during December and January. The PV term described in section 3.2.1 partially accounts for this enhancement. The ozone increase in this layer is likely to be related to STE processes in the UT. A striking result is that at neither site are there significant increases in MT ozone during the southern African biomass burning season, September-October (Fishman et al., 1991; Fishman et al., 1996; Thompson et al., 1996; Swap et al., 2002). One reason might be that predominant transport from the most heavily burning regions south of 20S at that time of year, tends to be southeast toward the Indian Ocean, not along a SA highveld to Réunion route (Swap et al., 2002; Kanyanga, 2009).

3.2 Possible Causes for Free Tropospheric Ozone Increase

We briefly investigate possible reasons for the ozone increases, considering dynamic factors and pollution sources.

3.2.1 Dynamical Considerations

The two sources of ozone in the FT are in situ chemical production and transport, where the former cause is generally believed to be at least several times greater than the latter (Stevenson et al., 2006). In this section we consider how meteorological parameters may influence both of these sources. Can the positive trends in TTL and FT ozone be explained by changes in the downward flow that transports ozone into the troposphere from the ozone-rich stratosphere during the wave-breaking process associated with Rossby wave activity (Collins et al., 2003)? Because PV is a convenient dynamical tracer of the stratospheric air parcels, we use it as a proxy for possible changes in STE events. We calculate monthly PV averages at both locations from the daily means of 12Z PV fields (for more details see section 2.3) and use these monthly averaged PV time series as a predictor in our regression model (Eq. 1). A similar approach (but with different goals) is used in Ziemke et al. (1997). Our results are indicated in **Figure 9**. Based on evaluating an ozone response to PV changes over Irene, **Figure 9a** shows a strong ozone sensitivity to a 330K

PV time series in September and October when frequent STE episodes associated with wave-breaking occur over the SA Highveld (Tyson et al., 1997) and when the ozone tropopause is at its lowest altitude (Sivakumar et al., 2011; Thompson et al., 2012). However, ozone changes at 9-11 km over Irene (corresponding to the 330K level) are only ~20%/decade in September and October, much less than the winter trends (**Figure 7**).

We examined 350K and 330K PV MJJA anomalies over Irene (derived from the monthly averaged PV time series described in section 2.3) for the 1990-2007 period to look for potential changes in STE activity during the MJJA period when the positive ozone trend is most evident (**Figure 10**). At the 350K level (**Figure 10a**) there is an indication of slightly decreasing PV; that would be consistent with findings of the well-characterized widening tropical belt (Seidel et al., 2008). However, such a perturbation would tend to favor a higher tropopause, fewer STE events and generally less ozone, opposite of what is observed (**Figure 7**). **Figure 10** also presents MJJA anomalies of tropospheric temperature and specific humidity over the 1990-2007 period. These are examined because it is known that up to 300 hPa (Collins et al., 2000) temperature increases may lead to higher water vapor (H_2O) mixing ratios and enhanced photochemical destruction of ozone through the series of reactions that form OH: $O_3 + hv + H_2O$. In **Figure 10** some temperature increases are evident, but there is no consistent, proportional response in specific humidity. Furthermore, if H_2O had increased in the 1990-2007 period, the tendency would be to suppress FT ozone, again the opposite of what is observed (**Figure 7**). We conclude that the evidence for dynamical change as the main driver for Irene FT winter ozone trends is not compelling.

At Réunion, a site decidedly more tropical than Irene, the STE effect (**Figure 9b**) is statistically significant only during December-January period in the 13-15 km layer corresponding to the 350K PV level (see Figure 3 in Thompson et al., 2012). Due to this sensitivity we think that the ozone changes in that layer during that time are tied to STE processes. **Figure 11** (green curve) suggests that PV influence on MT ozone (5-13 km) over Réunion is smaller than over Irene (**Figure 11**, blue curve), but STE events are known to occur at various times throughout the year (Baray et al., 1998; Randriambelo et al., 1999; Clain et al., 2010). In September and October tropical low pressure systems and the seasonal lowering of the tropopause are similar to Irene (Sivakumar et al., 2011). Greater PV values at Irene (**Figure 11,** blue curve) than at Réunion are not surprising given that Irene is closer to the southern hemispheric subtropical jet. Similar to Irene, we examined tropospheric PV, temperature, and specific humidity anomalies over Réunion for 1992-2011 (not shown) but did not find any noticeable changes.

In summary, there is some evidence for a dynamical role in UT ozone changes over Irene and Réunion, specifically during October-December at Irene and during December-January over Réunion. However, the large winter ozone trends at both locations do not seem to be explained by meteorology.

3.2.2 Photochemistry and Pollution

In a number of studies looking at southern African transport in September-October 1992, when intensive radiosonde and ozonesonde launches were made in Namibia and South Africa as part of Southern African Fire Atmospheric Research Initiative/Transport and Atmospheric Chemistry near the Equator-Atlantic, SAFARI-92/TRACE-A experiments

(e.g., Diab et al., 1996; Garstang et al., 1996; Thompson et al., 1996; Tyson et al., 1997), the Irene region was found to be in a transition region. Generally, north of 20S, easterlies took pollutants toward the Atlantic (Fishman et al., 1990; Fishman et al., 1996). On the SA Highveld, where Irene is located, flows in the mid-troposphere were often from the north or northeast, introducing layers of pollution from biomass fires, detected as elevated ozone (Thompson et al., 1996; Tyson et al., 1997). These layers recirculated and often exited Africa southeast toward the Indian Ocean where pollution was detected in aircraft sampling (Heikes et al., 1996). This transport pattern, designated the "river of smoke" as it appears in MODIS satellite imagery, was confirmed during SAFARI-2000 (Swap et al., 2003). In the mid-upper tropospheric transition zone, trajectories at 8-12 km showed many air parcels arriving over Irene during SAFARI-92/TRACE-A (Thompson et al., 1996) originated over South America. Irene soundings displayed ozone layers that resulted from South American biomass fire emissions that traveled toward Africa after they had been lofted to the UT by deep convection (Pickering et al., 1996; Thompson et al., 1997). This mechanism, augmented by NO from lightning (Smyth et al., 1996), was inferred from tracers measured on the DC-8 aircraft. Links between Réunion ozone and biomass fires over Africa and Madagascar are also well-established (Baldy et al., 1996; Randriambelo et al., 1999).

Figure 12, that displays air-parcel origins for the Irene and Réunion ozone soundings launched in May-August in 1992-2011, suggests that the springtime sources studied in SAFARI-92 and SAFARI-2000, also pertain to winter. Two levels are illustrated. For Irene (**Figure 12a**) the 500 hPa level trajectories (~5.5 km) are in the middle of the 4-7 km zone of +20-30%/decade ozone increase in May and June (**Figure 7**). The origins of the 500 hPa level air parcels over Irene are mainly located over the south Atlantic and eastern South America. For the 5-7 km ozone increases over Réunion (July and August in **Figure 8**), the change is also ~20%/decade. The origins of the corresponding air parcels over Réunion (**Figure 12c)** are concentrated over Madagascar, southern Africa and the eastern south Atlantic, where tropospheric ozone tends to accumulate year-round due to re-circulation within the south Atlantic gyre. Over five-day transit times from Irene at 300 hPa (**Figure 12b,** 150 hPa parcels, not shown, are similar), there is a high concentration of origins over South America as well as Africa and the south Atlantic (Fishman et al., 1990; Thompson et al., 2003; Jensen et al., 2012).

Réunion back-trajectories at 300 hPa (**Figure 12d**) in addition to South American, Atlantic and African origins, include air parcels from the tropical Indian Ocean, which is subject to pollution (Thompson et al., 2001; Chatfield et al., 2004). A study of sources and transport patterns of winter CO over Réunion (Duflot et al., 2010) shows that southern Africa and Madagascar, as well as South America, contribute to CO enhancement in the FT below 11 km. Back trajectory pathways, determined from FLEXPART, are similar to those illustrated in **Figures 12c,d.** Duflot et al. (2011) present MOPITT (Measurement of Pollution in the Troposphere) CO distributions observed over Réunion source regions. During June-August 2007 elevated CO over Réunion is linked to high-CO regions at 250 hPa over South America, the south Atlantic and southern Africa as well as southeast Asia and Indonesia. The CO sources are assumed to be predominantly anthropogenic. **Figure 12d** also suggests potential Réunion pollution sources from Southeast Asia. In September and

October there is a shift away from anthropogenic sources to more biomass burning CO, detected by MOPITT near the surface (Duflot et al., 2010) where Irene and Réunion (**Figures 7 and 8**) show no trend. The recent study of Zien et al. (2013) on NO_2 transport inferred from GOME-2 (Global Ozone Monitoring Experiment on MetOpA) in 2007-2011 gives a mostly similar picture to MOPITT. The largest NO_2 plumes in the southern hemisphere occur in JJA with origins densely concentrated over South America, southern Africa and the oceans to the southeast (Figures 15, 16, 19 in Zien et al., 2013). However, due to the shorter NO_2 lifetime, a link to southeast Asia and Indonesia does not appear.

Is there any evidence for increasing pollution over southern Africa and South America in the 1990-2011 period? The evidence is inconclusive. A recent study of global surface and lower tropospheric 20-40-yr trends by Oltmans et al. (2012) indicates that ozone at southern hemisphere monitoring stations is increasing, apparently due to anthropogenic activity. For Cape Point, SA, which experiences a wintertime brown haze, Oltmans et al. (2012; Figure 15) showed a ~25% surface ozone increase from 1990-2010, most of it in the 1990's. Our recent trends analysis of SA Highveld stations 50-125 km east and southeast of Irene (Balashov et al., 2014), showed little change in surface ozone or NO_x. Is there other evidence that would explain the large FT ozone increases seen in **Figures 7 and 8**? Satellite imagery of column NO_2 from SCIAMACHY (2002-2012. A. Richter and J. Burrows, personal communication, 2013) shows no significant change over south central Africa but a significant increase in a small region over the Highveld. **Figures 13** and **14** are based on standard emissions data (http://edgar.jrc.ec.europa.eu/index.php) that includes mobile transport, industrial, domestic and biomass fires. In general, biomass burning over Africa and South America does not appear to be increasing but industrial emissions are estimated to have increased over these continents 20-30% from 1990-2010. Our results are consistent with these values but suggest that they may be underestimates for winter.

In summary, it is hard to argue that FT ozone increases do not result partially from growing NO_x but further observations and source-tagged modeling are needed to better establish a link between changing emissions and the strongly seasonal ozone increases observed in the sonde record.

4. Summary and Conclusions

The Irene and Réunion free tropospheric ozonesonde records for 1990-2007 have been analyzed with a multi-variate regression model that accounts for the annual cycle, potential vorticity time series, and ENSO. In contrast to an earlier study (Clain et al., 2009), by using monthly averaged data, we are able to capture well-defined features throughout the annual cycle. Striking increases throughout the FT, 20-30%/decade over Irene and up to 50%/decade over Réunion, appear in winter (JJA), with smaller and more vertically diffuse increases in November and December. Below 5 km over Irene ozone has increased 15-25%/decade in late fall (April-June) and December. No statistically significant trends appear in September and October when biomass burning impacts on the South African Highveld are most pronounced. There are subtle differences between the Irene and Réunion ozone changes. The Irene increase starts in April or May and is concentrated between 4 and 8 km, almost separate from a June-July zone of ozone growth between 8 and 10.5 km. Over Réunion the ozone increase is largely confined to July and August, with a

single feature from 6-13 km. The mechanism(s) responsible for the ozone growth are not clear. Noting that both sites are in the influence of the subtropical jet, increases above 10 km are suggestive of dynamical changes near the tropopause. However, there is no clear evidence for the latter; indeed, likely changes in TTL properties would lead to ozone losses, not increases.

Mid-tropospheric ozone increases would be consistent with increases in southern hemisphere pollution. Trajectory analysis links Irene and Réunion air parcel origins to regions over Africa and the south Atlantic where ozone tends to accumulate throughout the year. At the 300 hPa level (9 km), air parcel origins extend over South America and the eastern Pacific. Estimated NO_x emissions increases, 20-30% from 1990-2010, would be consistent with the ozone trends observed over Irene and Réunion. However, surface ozone and NO_x trends over the SA Highveld in 1990 to 2007 do not appear to be consistent with such large growth. More observations are needed, along with a better knowledge of emissions. Model studies are called for as well as further studies of regional dynamics.

Acknowledgments. This study was begun during a Fulbright Scholar grant that allowed AMT to spend 8 months in South Africa during 2010-2011, with extraordinary support and hospitality from Northwest University-Potchefstroom (Dean J. J. Pienaar and his group), the CSIR-Pretoria (V. Sivakumar), the University of the Witwatersrand Climatology Research Group (S. J. Piketh) and co-author G. J. R. Coetzee (South African Weather Service). Helpful comments on the manuscript were received from D. Waugh (Johns Hopkins Univ.), J.-L. Baray (LaMP/OPGC, France) and from L. D. Oman and S. Strode at NASA/GSFC. Irene sondes are made possible by the South African Weather Service. The sonde program at Réunion is supported by CNRS and SHADOZ with technical assistance from NOAA/Global Monitoring Division (GMD; S. J. Oltmans and B. J. Johnson). SHADOZ has been funded since 1998 by the Upper Atmosphere Research Program of NASA (thanks to M. J. Kurylo and K. W. Jucks) with contributions from NOAA/GMD and NASA's Aura Validation. Support for this analysis came from grants to the Pennsylvania State University: NNG05GP22G, NNG05GO62G and NNX09AJ23G. The authors acknowledge the strong support of the European Commission, Airbus, and the Airlines (Lufthansa, Air-France, Austrian, Air Namibia, Cathay Pacific and China Airlines so far) who carry the MOZAIC or IAGOS equipment and performed the maintenance since 1994. MOZAIC is presently funded by INSU-CNRS (France), Météo-France, CNES, Université Paul Sabatier (Toulouse, France) and Research Center Jülich (FZJ, Jülich, Germany). IAGOS has been additionally funded by the EU projects IAGOS-DS and IAGOS-ERI. The MOZAIC-IAGOS data are available via CNES/CNRS-INSU Ether web site http://www.pole-ether.fr

FIGURE CAPTIONS

Figure 1. Location of Irene soundings and Johannesburg MOZAIC landing/takeoff profiles (blue star) and Réunion soundings (red star). Also illustrated are typical recirculation patterns over southern Africa and an outflow route to the Indian Ocean (maroon arrows). Flows toward the southern African region and eastern Indian Ocean from South America and southern Asia are indicated by blue arrows (see Figure 12).

Figure 2. Seasonal cycle of free and upper tropospheric ozone over Irene, based on monthly averages for two periods of observations for Irene and Réunion: (a) Irene sondes from 4-15 km (1990-1993,1999) with MOZAIC ozone from 4-11 km (1995-1999); (b) Irene (SHADOZ) sondes from 2000-2007, 2012-2013; (c) Réunion (pre-SHADOZ and SHADOZ) sondes launched in 1992-2001; (d)

Réunion (SHADOZ) sondes from 2002-2011.

Figure 3. (a) Ozone mixing ratio, averaged 4-15 km, from the Réunion Island sonde record that started in 1992. (b) corresponding data frequency of profiles used in (a) by month.

Figure 4. (a) Launch times for Irene, South Africa (25.9S, 28.2E) balloon-borne ozonesonde-radiosonde packages during 1990-1993 (blue) and for SHADOZ from 1999 to early 2007 (green). (b) Mean ozone mixing ratio in the 1.5-4 km layer from Irene sondes corresponding to the sampling times in (a), showing the upward trend in ozone mixing ratio as launch times moved later in the day. (c) Correlation between sonde launch times and ozone mixing ratio from the time-series in (a and b) as a function of altitude in 0.1 km bins from the surface (1.5 km) to 11 km.

Figure 5. Difference between Irene ozonesonde climatology combined from 1990-1993, 1999-2007 and MOZAIC climatology from 1995-1999. Hatched areas represent statistically significant deviations of climatologies (places where a standard deviation values from two climatologies do not overlap).

Figure 6. (a) Ozone mixing ratio averaged 4-11 km, from the earlier (1990-1993) Irene record (blue) and the SHADOZ Irene period (1999-2007) (green). The red dots depict averaged ozone mixing ratio, 4-11 km, from MOZAIC profiles acquired in 1995-1998 from an instrumented commercial jet during landings and takeoffs (LTO) at Johannesburg (JNB, O. R. Thambo) airport (Thouret et al., 1998; 2012; Clain et al. 2009). The magenta dots represent the combined record of MOZAIC and SHADOZ. (b) corresponding data frequency of profiles used in (a) by month for Irene and JNB. Equipment changes by the airlines have interrupted the commercial aircraft ozone sampling project in MOZAIC (now IAGOS). Two field campaigns (SAFARI-92/TRACE-A in September-October 1992; Diab et al., 1996; Thompson et al., 1996) and SAFARI-2000 in September 2000 (Swap et al., 2003; Thompson et al., 2002) gave rise to more frequent Irene launches.

Figure 7. Trend (change in %/decade) computed from multivariate regression model for combined 4-11 km, Irene-JNB MOZAIC profile data, 1990-2007. Diagonal shading denotes statistical significance. Increases below 5 km may be related to surface pollution. Note that losses (blue in F-M-A and September-October) are not statistically significant.

Figure 8. Same as **Figure 7** except trend in Réunion profiles, 4-15 km, from 1992-2011.

Figure 9. (a) Irene tropospheric ozone (4-11 km layer) sensitivity toward the 330K

potential vorticity time series (ppbv/1 PV unit) over the box bounded by 25.5º-32.2º S and 24.8º-31.5º E for 1990-2007. (b) Réunion tropospheric ozone (4-15 km layer) sensitivity toward the 350K potential vorticity time series (ppbv/1 PV unit) over the box bounded by 18º-25º S and 49.5º-65.25º E for 1992-2011. Statistically significant response is shaded. Note that the altitude scales are different for the stations.

Figure 10. Irene (25.5º-32.2º S; 24.8º-31.5º E) MJJA temperature (T) and specific humidity (q) anomalies for 4 pressure levels and potential vorticity (PV) anomalies for 2 isotropic levels.

Figure 11. ECMWF potential vorticity (PV) daily climatologies over Irene for 330K and Réunion for 330K and 350K calculated, respectively, over 1990-2007 and 1992-2011, by averaging day-of-year values.

Figure 12. Air mass origins of free tropospheric ozone over Irene (a for the sonde launch time at 500 hPa, b for 300 hPa) and Réunion (c,d). Five-day back trajectories run using NCEP/NCAR re-analysis in the NASA/Goddard kinematic model are used. The ending points are summed up for a 1x1-degree grid. Note different color bars for the two sites.

Figure 13. EDGAR annual emissions (total country EDGAR V4.2 emissions from http://edgar.jrc.ec.europa.eu/index.php), in Gg (gigagrams) of the principal tropospheric ozone precursors (a) nitrogen oxides (NO_x), (b) carbon monoxide (CO), and (c) non-methane volatile organic compounds (NMVOC) over selected African countries that correspond to trajectory origins in **Figure 12**.

Figure 14. Same as **Figure 13** except for selected South American countries: Bolivia, Brazil, Paraguay, and Uruguay. The countries were chosen based on the trajectories in **Figure 12**.

REFERENCES

Balashov, N. V., Thompson, A. M., Piketh, S. J., and Langerman, K. E.: Surface ozone variability and trends over the South African Highveld from 1990 to 2007, Journal of Geophysical Research: Atmospheres, 119, 4323–4342, 10.1002/2013jd020555, 2014.

Baldy, S., Ancellet, G., Bessafi, M., Badr, A., and Luk, D. L. S.: Field observations of the vertical distribution of tropospheric ozone at the island of Reunion (southern tropics), Journal of Geophysical Research: Atmospheres, 101, 23835-23849, 10.1029/95jd02929, 1996.

Baray, J. L., Ancellet, G., Taupin, F. G., Bessafi, M., Baldy, S., and Keckhut, P.: Subtropical tropopause break as a possible stratospheric source of ozone in the tropical troposphere,

573 Journal of Atmospheric and Solar-Terrestrial Physics, 60, 27-36,
574 http://dx.doi.org/10.1016/S1364-6826(97)00116-8, 1998.
575 Baray, J. L., Leveau, J., Baldy, S., Jouzel, J., Keckhut, P., Bergametti, G., Ancellet, G.,
576 Bencherif, H., Cadet, B., Carleer, M., David, C., De Maziere, M., Faduilhe, D.,
577 Beekmann, S. G., Goloub, P., Goutail, F., Metzger, J. M., Morel, B., Pommereau, J. P.,
578 Porteneuve, J., Portafaix, T., Posny, F., Robert, L., and Van Roozendael, M.: An
579 instrumented station for the survey of ozone and climate change in the southern tropics, J.
580 Environ. Monit., 8, 1020-1028, 10.1039/b607762e, 2006.
581 Beekmann, M., Ancellet, G., and Megie, G.: Climatology of tropospheric ozone in southern
582 Europe and its relation to potential vorticity, J. Geophys. Res.-Atmos., 99, 12841-12853,
583 10.1029/94jd00228, 1994.
584 Beig, G., and Singh, V.: Trends in tropical tropospheric column ozone from satellite data and
585 MOZART model, Geophysical Research Letters, 34, L17801, 10.1029/2007gl030460,
586 2007.
587 Brunekreef, B., and Holgate, S. T.: Air pollution and health, The lancet, 360, 1233-1242, 2002.
588 Chandra, S., Ziemke, J. R., Min, W., and Read, W. G.: Effects of 1997–1998 El Niño on
589 tropospheric ozone and water vapor, Geophysical Research Letters, 25, 3867-3870,
590 10.1029/98gl02695, 1998.
591 Chatfield, R. B., Guan, H., Thompson, A. M., and Witte, J. C.: Convective lofting links Indian
592 Ocean air pollution to paradoxical South Atlantic ozone maxima, Geophys. Res. Lett., 31,
593 L06103, doi:10.1029/2003gl018866, 2004.
594 Clain, G., Baray, J. L., Delmas, R., Diab, R., de Bellevue, J. L., Keckhut, P., Posny, F., Metzger,
595 J. M., and Cammas, J. P.: Tropospheric ozone climatology at two Southern Hemisphere
596 tropical/subtropical sites, (Reunion Island and Irene, South Africa) from ozonesondes,
597 LIDAR, and in situ aircraft measurements, Atmos. Chem. Phys., 9, 1723-1734, 2009.
598 Clain, G., Baray, J. L., Delmas, R., Keckhut, P., and Cammas, J. P.: A lagrangian approach to
599 analyse the tropospheric ozone climatology in the tropics: Climatology of stratosphere-
600 troposphere exchange at Reunion Island, Atmospheric Environment, 44, 968-975,
601 10.1016/j.atmosenv.2009.08.048, 2010.
602 Collins, W. J., Derwent, R. G., Johnson, C. E., and Stevenson, D. S.: The impact of human
603 activities on the photochemical production and destruction of tropospheric ozone, Q. J. R.
604 Meteorol. Soc., 126, 1925-1951, 10.1256/smsqj.56618, 2000.
605 Collins, W. J., Derwent, R. G., Garnier, B., Johnson, C. E., Sanderson, M. G., and Stevenson, D.
606 S.: Effect of stratosphere-troposphere exchange on the future tropospheric ozone trend, J.
607 Geophys. Res.-Atmos., 108, 8528, doi:10.1029/2002jd002617, 2003.
608 Cooper, O. R., Gao, R. S., Tarasick, D., Leblanc, T., and Sweeney, C.: Long-term ozone trends
609 at rural ozone monitoring sites across the United States, 1990–2010, J. Geophys. Res.
610 Atmos., 117, D22307, doi:10.1029/2012jd018261, 2012.
611 Dee, D. P., Uppala, S. M., Simmons, A. J., Berrisford, P., Poli, P., Kobayashi, S., Andrae, U.,
612 Balmaseda, M. A., Balsamo, G., Bauer, P., Bechtold, P., Beljaars, A. C. M., van de Berg,
613 L., Bidlot, J., Bormann, N., Delsol, C., Dragani, R., Fuentes, M., Geer, A. J., Haimberger,
614 L., Healy, S. B., Hersbach, H., Holm, E. V., Isaksen, L., Kallberg, P., Kohler, M.,
615 Matricardi, M., McNally, A. P., Monge-Sanz, B. M., Morcrette, J. J., Park, B. K., Peubey,
616 C., de Rosnay, P., Tavolato, C., Thepaut, J. N., and Vitart, F.: The ERA-Interim

reanalysis: configuration and performance of the data assimilation system, Q. J. R. Meteorol. Soc., 137, 553-597, 10.1002/qj.828, 2011.
Diab, R. D., Thompson, A. M., Zunckel, M., Coetzee, G. J. R., Combrink, J., Bodeker, G. E., Fishman, J., Sokolic, F., McNamara, D. P., Archer, C. B., and Nganga, D.: Vertical ozone distribution over southern Africa and adjacent oceans during SAFARI-92, Journal of Geophysical Research: Atmospheres, 101, 23823-23833, 10.1029/96jd01267, 1996.
Diab, R. D., Raghunandan, A., Thompson, A. M., and Thouret, V.: Classification of tropospheric ozone profiles over Johannesburg based on mozaic aircraft data, Atmos. Chem. Phys., 3, 713-723, 10.5194/acp-3-713-2003, 2003.
Diab, R. D., Thompson, A. M., Mari, K., Ramsay, L., and Coetzee, G. J. R.: Tropospheric ozone climatology over Irene, South Africa, from 1990 to 1994 and 1998 to 2002, J. Geophys. Res.-Atmos., 109, D20301, doi:10.1029/2004jd004793, 2004.
Doughty, D. C., Thompson, A. M., Schoeberl, M. R., Stajner, I., Wargan, K., and Hui, W. C. J.: An intercomparison of tropospheric ozone retrievals derived from two Aura instruments and measurements in western North America in 2006, Journal of Geophysical Research: Atmospheres, 116, D06303, 10.1029/2010jd014703, 2011.
Duflot, V., Dils, B., Baray, J. L., De Maziere, M., Attie, J. L., Vanhaelewyn, G., Senten, C., Vigouroux, C., Clain, G., and Delmas, R.: Analysis of the origin of the distribution of CO in the subtropical southern Indian Ocean in 2007, J. Geophys. Res.-Atmos., 115, D22106, doi:10.1029/2010jd013994, 2010.
Duflot, V., Royer, P., Chazette, P., Baray, J. L., Courcoux, Y., and Delmas, R.: Marine and biomass burning aerosols in the southern Indian Ocean: Retrieval of aerosol optical properties from shipborne lidar and Sun photometer measurements, J. Geophys. Res.-Atmos., 116, 10.1029/2011jd015839, 2011.
Fishman, J., Watson, C. E., Larsen, J. C., and Logan, J. A.: Distribution of tropospheric ozone determined from satellite data, Journal of Geophysical Research: Atmospheres, 95, 3599-3617, 10.1029/JD095iD04p03599, 1990.
Fishman, J., FAKHRUZZAMAN, K., CROS, B., and NGANGA, D.: Identification of Widespread Pollution in the Southern Hemisphere Deduced from Satellite Analyses, Science, 252, 1693-1696, 10.1126/science.252.5013.1693, 1991.
Fishman, J., Brackett, V. G., Browell, E. V., and Grant, W. B.: Tropospheric ozone derived from TOMS/SBUV measurements during TRACE A, Journal of Geophysical Research: Atmospheres, 101, 24069-24082, 10.1029/95jd03576, 1996.
Fujiwara, M., Kita, K., Kawakami, S., Ogawa, T., Komala, N., Saraspriya, S., and Suripto, A.: Tropospheric ozone enhancements during the Indonesian Forest Fire Events in 1994 and in 1997 as revealed by ground-based observations, Geophysical Research Letters, 26, 2417-2420, 10.1029/1999gl900117, 1999.
Gallardo, L., Alonso, M., Andrade, M. deF., Barreto Carvalho, V. S., Behrentz, E., de Castro Vasconcellos, P., D'Angiola, A., Dawidowski, L., Freitas, S., Gómez, D., Longo, K. M., Doprichinski Martins, L., Mena, M., Matus, P., Osses, A., Osses, M., Rojas, N., Saide, P., Sánchez-Ccoyllo, O., Toro, M. V., South America, in in: WMO/IGAC Impacts Of Megacities On Air Pollution and Climate, edited by: Zhu, T., Melamed, M. L., Parrish, D., Gauss, M., Klenner, L. G., Lawrence, M., Konaré, A., and Liousse, C., World Meteorological Organization (WMO), Geneva, 28-58, 2012.

Garstang, M., Tyson, P. D., Swap, R., Edwards, M., Kållberg, P., and Lindesay, J. A.: Horizontal and vertical transport of air over southern Africa, Journal of Geophysical Research: Atmospheres, 101, 23721-23736, 10.1029/95jd00844, 1996.

Heikes, B., Lee, M., Jacob, D., Talbot, R., Bradshaw, J., Singh, H., Blake, D., Anderson, B., Fuelberg, H., and Thompson, A. M.: Ozone, hydroperoxides, oxides of nitrogen, and hydrocarbon budgets in the marine boundary layer over the South Atlantic, Journal of Geophysical Research: Atmospheres, 101, 24221-24234, 10.1029/95jd03631, 1996.

Holton, J. R., Haynes, P. H., McIntyre, M. E., Douglass, A. R., Rood, R. B., and Pfister, L.: Stratosphere-troposphere exchange Rev. Geophys., 33, 403-439, 10.1029/95rg02097, 1995.

Jensen, A. A., Thompson, A. M., and Schmidlin, F. J.: Classification of Ascension Island and Natal ozonesondes using self-organizing maps, Journal of Geophysical Research: Atmospheres, 117, D04302, 10.1029/2011jd016573, 2012.

Johnson, B. J., Oltmans, S. J., Vömel, H., Smit, H. G. J., Deshler, T., and Kröger, C.: Electrochemical concentration cell (ECC) ozonesonde pump efficiency measurements and tests on the sensitivity to ozone of buffered and unbuffered ECC sensor cathode solutions, Journal of Geophysical Research: Atmospheres, 107, 4393, 10.1029/2001jd000557, 2002.

Kanyanga, J. K.: El Niño Southern Oscillation (ENSO) and Atmospheric Transport over Southern Africa, Unpublished PhD Thesis, University of Johannesburg, South Africa, 2008.

Keyser, D., and Shapiro, M. A.: A review of the structure and dynamics of upper-level frontal zones, Mon. Weather Rev., 114, 452-499, 10.1175/1520-0493(1986)114<0452:arotsa>2.0.co;2, 1986.

Lee, S., Shelow, D. M., Thompson, A. M., and Miller, S. K.: QBO and ENSO variability in temperature and ozone from SHADOZ, 1998–2005, J. Geophys. Res.-Atmos., 115, D18105, doi:10.1029/2009JD013320, 2010.

Liousse, C., Konaré, A., Kanakidou, M., and Pienaar, K.: Africa, in: WMO/IGAC Impacts Of Megacities On Air Pollution and Climate, edited by: Zhu, T., Melamed, M. L., Parrish, D., Gauss, M., Klenner, L. G., Lawrence, M., Konaré, A., and Liousse, C., World Meteorological Organization (WMO), Geneva, 28-58, 2012.

Liousse, C., Assamoi, E., Criqui, P., Granier, C., Rosset, R., Explosive growth in African combustion emissions from 2005 to 2030, Enviorn. Res. Lett., 9, doi:10.1088/1748-9326/9/3/035003, 2014.

Logan, J. A., Megretskaia, I., Nassar, R., Murray, L. T., Zhang, L., Bowman, K. W., Worden, H. M., and Luo, M.: Effects of the 2006 El Niño on tropospheric composition as revealed by data from the Tropospheric Emission Spectrometer (TES), Geophysical Research Letters, 35, L03816, 10.1029/2007gl031698, 2008.

Logan, J. A., Staehelin, J., Megretskaia, I. A., Cammas, J. P., Thouret, V., Claude, H., De Backer, H., Steinbacher, M., Scheel, H. E., Stübi, R., Fröhlich, M., and Derwent, R.: Changes in ozone over Europe: Analysis of ozone measurements from sondes, regular aircraft (MOZAIC) and alpine surface sites, Journal of Geophysical Research: Atmospheres, 117, D09301, 10.1029/2011jd016952, 2012.

Lourens, A. S., Beukes, J. P., van Zyl, P. G., Fourie, G. D., Burger, J. W., Pienaar, J. J., Read, C. E., and Jordaan, J. H.: Spatial and temporal assessment of gaseous pollutants in the

706 Highveld of South Africa, South African Journal of Science, 107, 55-62,
707 10.4102/sajs.v107i1/2.269, 2011.
708 Oltmans, S., Lefohn, A., Shadwick, D., Harris, J., Scheel, H., Galbally, I., Tarasick, D., Johnson,
709 B., Brunke, E.-G., and Claude, H.: Recent tropospheric ozone changes – a pattern
710 dominated by slow or no growth, Atmos. Environ., 67, 331–351,
711 doi:10.1016/j.atmosenv.2012.10.057, 2013.
712 Oman, L. D., Ziemke, J. R., Douglass, A. R., Waugh, D. W., Lang, C., Rodriguez, J. M., and
713 Nielsen, J. E.: The response of tropical tropospheric ozone to ENSO, Geophysical
714 Research Letters, 38, L13706, 10.1029/2011gl047865, 2011.
715 Parrish, D. D., Law, K. S., Staehelin, J., Derwent, R., Cooper, O. R., Tanimoto, H., Volz-
716 Thomas, A., Gilge, S., Scheel, H. E., Steinbacher, M., and Chan, E.: Long-term changes
717 in lower tropospheric baseline ozone concentrations at northern mid-latitudes, Atmos.
718 Chem. Phys., 12, 11485-11504, 10.5194/acp-12-11485-2012, 2012.
719 Parrish, D. D., Law, K. S., Staehelin, J., Derwent, R., Cooper, O. R., Tanimoto, H., Volz-
720 Thomas, A., Gilge, S., Scheel, H. E., Steinbacher, M., and Chan, E.: Lower tropospheric
721 ozone at northern midlatitudes: Changing seasonal cycle, Geophysical Research Letters,
722 40, 1631-1636, 10.1002/grl.50303, 2013.
723 Pickering, K. E., Thompson, A. M., Wang, Y., Tao, W.-K., McNamara, D. P., Kirchhoff, V. W.
724 J. H., Heikes, B. G., Sachse, G. W., Bradshaw, J. D., Gregory, G. L., and Blake, D. R.:
725 Convective transport of biomass burning emissions over Brazil during TRACE A,
726 Journal of Geophysical Research: Atmospheres, 101, 23993-24012, 10.1029/96jd00346,
727 1996.
728 Randel, W. J., and Cobb, J. B.: Coherent variations of monthly mean total ozone and lower
729 stratospheric temperature, Journal of Geophysical Research: Atmospheres, 99, 5433-
730 5447, 10.1029/93jd03454, 1994.
731 Randel, W. J., and Thompson, A. M.: Interannual variability and trends in tropical ozone derived
732 from SAGE II satellite data and SHADOZ ozonesondes, Journal of Geophysical
733 Research: Atmospheres, 116, D07303, 10.1029/2010jd015195, 2011.
734 Randriambelo, T., Baray, J. L., Baldy, S., Bremaud, P., and Cautenet, S.: A case study of
735 extreme tropospheric ozone contamination in the tropics using in-situ, satellite and
736 meteorological data, Geophysical Research Letters, 26, 1287-1290,
737 10.1029/1999gl900229, 1999.
738 Rao, T. N., Kirkwood, S., Arvelius, J., von der Gathen, P., and Kivi, R.: Climatology of UTLS
739 ozone and the ratio of ozone and potential vorticity over northern Europe, J. Geophys.
740 Res.-Atmos., 108(D22), 4703, doi:10.1029/2003jd003860, 2003.
741 Rorich, R. P., and Galpin, J. S.: Air quality in the Mpumalanga Highveld region, South Africa,
742 South African Journal of Science, 94, 109-114, 1998.
743 Schoeberl, M. R., Ziemke, J. R., Bojkov, B., Livesey, N., Duncan, B., Strahan, S., Froidevaux,
744 L., Kulawik, S., Bhartia, P. K., Chandra, S., Levelt, P. F., Witte, J. C., Thompson, A. M.,
745 Cuevas, E., Redondas, A., Tarasick, D. W., Davies, J., Bodeker, G., Hansen, G., Johnson,
746 B. J., Oltmans, S. J., Vömel, H., Allaart, M., Kelder, H., Newchurch, M., Godin-
747 Beekmann, S., Ancellet, G., Claude, H., Andersen, S. B., Kyrö, E., Parrondos, M., Yela,
748 M., Zablocki, G., Moore, D., Dier, H., von der Gathen, P., Viatte, P., Stübi, R., Calpini,
749 B., Skrivankova, P., Dorokhov, V., de Backer, H., Schmidlin, F. J., Coetzee, G.,
750 Fujiwara, M., Thouret, V., Posny, F., Morris, G., Merrill, J., Leong, C. P., Koenig-

Langlo, G., and Joseph, E.: A trajectory-based estimate of the tropospheric ozone column using the residual method, Journal of Geophysical Research: Atmospheres, 112, D24S49, 10.1029/2007jd008773, 2007.
Seidel, D. J., Fu, Q., Randel, W. J., and Reichler, T. J.: Widening of the tropical belt in a changing climate, Nat. Geosci., 1, 21-24, 10.1038/ngeo.2007.38, 2008.
Shindell, D., Faluvegi, G., Lacis, A., Hansen, J., Ruedy, R., and Aguilar, E.: Role of tropospheric ozone increases in 20th-century climate change, J. Geophys. Res.-Atmos., 111, D08302, doi:10.1029/2005jd006348, 2006.
Sivakumar, V., Bencherif, H., Bègue, N., and Thompson, A. M.: Tropopause Characteristics and Variability from 11 yr of SHADOZ Observations in the Southern Tropics and Subtropics, Journal of Applied Meteorology and Climatology, 50, 1403-1416, 10.1175/2011jamc2453.1, 2011.
Smit, H. and the ASOPOS Panel.: Quality Assurance and Quality Control for Ozonesonde Measurements in GAW, WMO/GAW Rep, 201, Geneva**,** Switzerland, 2011. www.wmo.int/pages/prog/arep/gaw/gaw-reports.html
Smit, H. G. J., Straeter, W., Johnson, B. J., Oltmans, S. J., Davies, J., Tarasick, D. W., Hoegger, B., Stubi, R., Schmidlin, F. J., Northam, T., Thompson, A. M., Witte, J. C., Boyd, I., and Posny, F.: Assessment of the performance of ECC-ozonesondes under quasi-flight conditions in the environmental simulation chamber: Insights from the Juelich Ozone Sonde Intercomparison Experiment (JOSIE), Journal of Geophysical Research: Atmospheres, 112, D19306, 10.1029/2006jd007308, 2007.
Smyth, S. B., Sandholm, S. T., Bradshaw, J. D., Talbot, R. W., Blake, D. R., Blake, N. J., Rowland, F. S., Singh, H. B., Gregory, G. L., Anderson, B. E., Sachse, G. W., Collins, J. E., and Bachmeier, A. S.: Factors influencing the upper free tropospheric distribution of reactive nitrogen over the South Atlantic during the TRACE A experiment, J. Geophys. Res.-Atmos., 101, 24165-24186, 10.1029/96jd00224, 1996.
Stajner, I., Wargan, K., Pawson, S., Hayashi, H., Chang, L.-P., Hudman, R. C., Froidevaux, L., Livesey, N., Levelt, P. F., Thompson, A. M., Tarasick, D. W., Stübi, R., Andersen, S. B., Yela, M., König-Langlo, G., Schmidlin, F. J., and Witte, J. C.: Assimilated ozone from EOS-Aura: Evaluation of the tropopause region and tropospheric columns, Journal of Geophysical Research: Atmospheres, 113, D16S32, 10.1029/2007jd008863, 2008.
Stevenson, D. S., Dentener, F. J., Schultz, M. G., et al.: Multimodel ensemble simulations of present-day and near-future tropospheric ozone, J. Geophys. Res.-Atmos., 111, D08301, doi:10.1029/2005jd006338, 2006.
Swap, R., Annegarn, H., Suttles, J., Haywood, J., Helmlinger, M., Hely, C., Hobbs, P., Holben, B., Ji, J., and King, M.: The Southern African Regional Science Initiative (SAFARI 2000): overview of the dry season field campaign, South African Journal of Science, 98, 125-130, 2002.
Swap, R. J., Annegarn, H. J., Suttles, J. T., King, M. D., Platnick, S., Privette, J. L., and Scholes, R. J.: Africa burning: A thematic analysis of the Southern African Regional Science Initiative (SAFARI 2000), Journal of Geophysical Research: Atmospheres, 108, 8465, 10.1029/2003jd003747, 2003.
Thompson, A. M., Diab, R. D., Bodeker, G. E., Zunckel, M., Coetzee, G. J. R., Archer, C. B., McNamara, D. P., Pickering, K. E., Combrink, J., Fishman, J., and Nganga, D.: Ozone

795 over southern Africa during SAFARI-92/TRACE A, Journal of Geophysical Research:
796 Atmospheres, 101, 23793-23807, 10.1029/95jd02459, 1996.
797 Thompson, A. M., Tao, W.-K., Pickering, K. E., Scala, J. R., and Simpson, J.: Tropical Deep
798 Convection and Ozone Formation, Bulletin of the American Meteorological Society, 78,
799 1043-1054, 10.1175/1520-0477(1997)078<1043:tdcaof>2.0.co;2, 1997.
800 Thompson, A. M., and Hudson, R. D.: Tropical tropospheric ozone (TTO) maps from Nimbus 7
801 and Earth Probe TOMS by the modified-residual method: Evaluation with sondes, ENSO
802 signals, and trends from Atlantic regional time series, Journal of Geophysical Research:
803 Atmospheres, 104, 26961-26975, 10.1029/1999jd900470, 1999.
804 Thompson, A. M., Witte, J. C., Hudson, R. D., Guo, H., Herman, J. R., and Fujiwara, M.:
805 Tropical Tropospheric Ozone and Biomass Burning, Science, 291, 2128-2132,
806 10.1126/science.291.5511.2128, 2001.
807 Thompson, A. M., Witte, J. C., Freiman, M. T., Phahlane, N. A., and Coetzee, G. J. R.: Lusaka,
808 Zambia, during SAFARI-2000: Convergence of local and imported ozone pollution,
809 Geophysical Research Letters, 29, 1976, 10.1029/2002gl015399, 2002.
810 Thompson, A. M., Witte, J. C., McPeters, R. D., Oltmans, S. J., Schmidlin, F. J., Logan, J. A.,
811 Fujiwara, M., Kirchhoff, V. W. J. H., Posny, F., Coetzee, G. J. R., Hoegger, B.,
812 Kawakami, S., Ogawa, T., Johnson, B. J., Vömel, H., and Labow, G.: Southern
813 Hemisphere Additional Ozonesondes (SHADOZ) 1998–2000 tropical ozone climatology
814 1. Comparison with Total Ozone Mapping Spectrometer (TOMS) and ground-based
815 measurements, Journal of Geophysical Research: Atmospheres, 108, 8238,
816 10.1029/2001jd000967, 2003.
817 Thompson, A. M., Stone, J. B., Witte, J. C., Miller, S. K., Pierce, R. B., Chatfield, R. B.,
818 Oltmans, S. J., Cooper, O. R., Loucks, A. L., Taubman, B. F., Johnson, B. J., Joseph, E.,
819 Kucsera, T. L., Merrill, J. T., Morris, G. A., Hersey, S., Forbes, G., Newchurch, M. J.,
820 Schmidlin, F. J., Tarasick, D. W., Thouret, V., and Cammas, J.-P.: Intercontinental
821 chemical transport experiment ozonesonde network study (IONS) 2004: 1. Summertime
822 upper troposphere/lower stratosphere ozone over northeastern North America, J.
823 Geophys. Res.-Atmos., 112, D12S12, doi:10.1029/2006JD007441, 2007.
824 Thompson, A. M., Allen, A. L., Lee, S., Miller, S. K., and Witte, J. C.: Gravity and Rossby wave
825 signatures in the tropical troposphere and lower stratosphere based on Southern
826 Hemisphere Additional Ozonesondes (SHADOZ), 1998–2007, J. Geophys. Res.-Atmos.,
827 116, D05302, doi:10.1029/2009JD013429, 2011.
828 Thompson, A. M., Miller, S. K., Tilmes, S., Kollonige, D. W., Witte, J. C., Oltmans, S. J.,
829 Johnson, B. J., Fujiwara, M., Schmidlin, F. J., Coetzee, G. J. R., Komala, N., Maata, M.,
830 bt Mohamad, M., Nguyo, J., Mutai, C., Ogino, S. Y., Da Silva, F. R., Leme, N. M. P.,
831 Posny, F., Scheele, R., Selkirk, H. B., Shiotani, M., Stübi, R., Levrat, G., Calpini, B.,
832 Thouret, V., Tsuruta, H., Canossa, J. V., Vömel, H., Yonemura, S., Diaz, J. A., Tan
833 Thanh, N. T., and Thuy Ha, H. T.: Southern Hemisphere Additional Ozonesondes
834 (SHADOZ) ozone climatology (2005–2009): Tropospheric and tropical tropopause layer
835 (TTL) profiles with comparisons to OMI-based ozone products, Journal of Geophysical
836 Research: Atmospheres, 117, D23301, 10.1029/2011jd016911, 2012.
837 Thouret, V., Marenco, A., Logan, J. A., Nedelec, P., and Grouhel, C.: Comparisons of ozone
838 measurements from the MOZAIC airborne program and the ozone sounding network at
839 eight locations, J. Geophys. Res.-Atmos., 103, 25695-25720, 10.1029/98jd02243, 1998.

Tyson, P. D., Garstang, M., Thompson, A. M., D'Abreton, P., Diab, R. D., and Browell, E. V.: Atmospheric transport and photochemistry of ozone over central Southern Africa during the Southern Africa Fire-Atmosphere Research Initiative, Journal of Geophysical Research: Atmospheres, 102, 10623-10635, 10.1029/97jd00170, 1997.

van der A, R. J., Eskes, H. J., Boersma, K. F., van Noije, T. P. C., Van Roozendael, M., De Smedt, I., Peters, D., and Meijer, E. W.: Trends, seasonal variability and dominant NO_x source derived from a ten year record of NO_2 measured from space, J. Geophys. Res.-Atmos., 113, *D04302*, doi:10.1029/2007jd009021, 2008.

Wilks, D. S.: Resampling Hypothesis Tests for Autocorrelated Fields, Journal of Climate, 10, 65-82, 10.1175/1520-0442(1997)010<0065:rhtfaf>2.0.co;2, 1997.

Ziemke, J. R., Chandra, S., McPeters, R. D., and Newman, P. A.: Dynamical proxies of column ozone with applications to global trend models, Journal of Geophysical Research: Atmospheres, 102, 6117-6129, 10.1029/96jd03783, 1997.

Zien, A. W., Richter, A., Hilboll, A., Blechschmidt, A. M., and Burrows, J. P.: Systematic analysis of tropospheric NO_2 long-range transport events detected in GOME-2 satellite data, Atmos. Chem. Phys. Discuss., 13, 30945-31012, 10.5194/acpd-13-30945-2013, 2013.

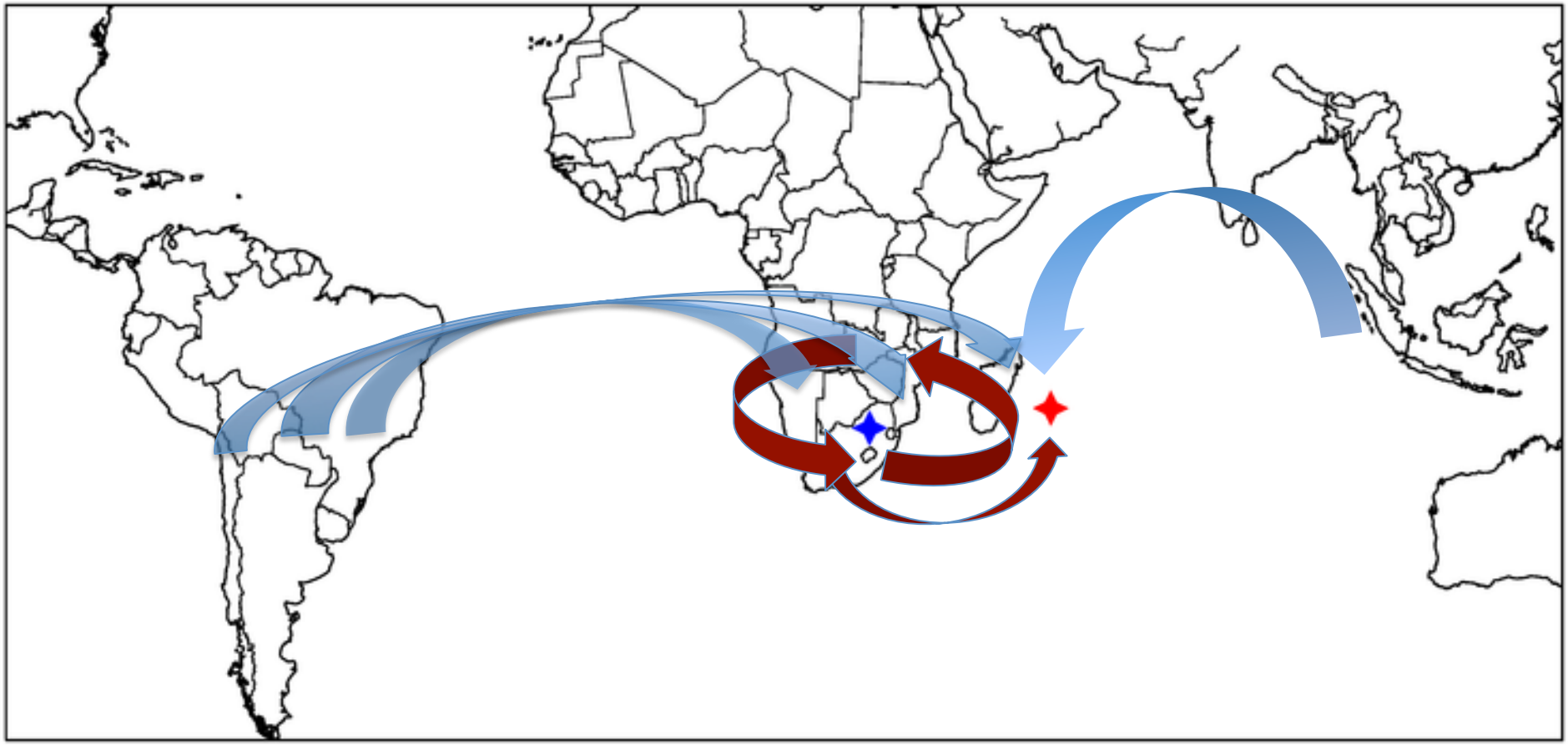

Figure 1

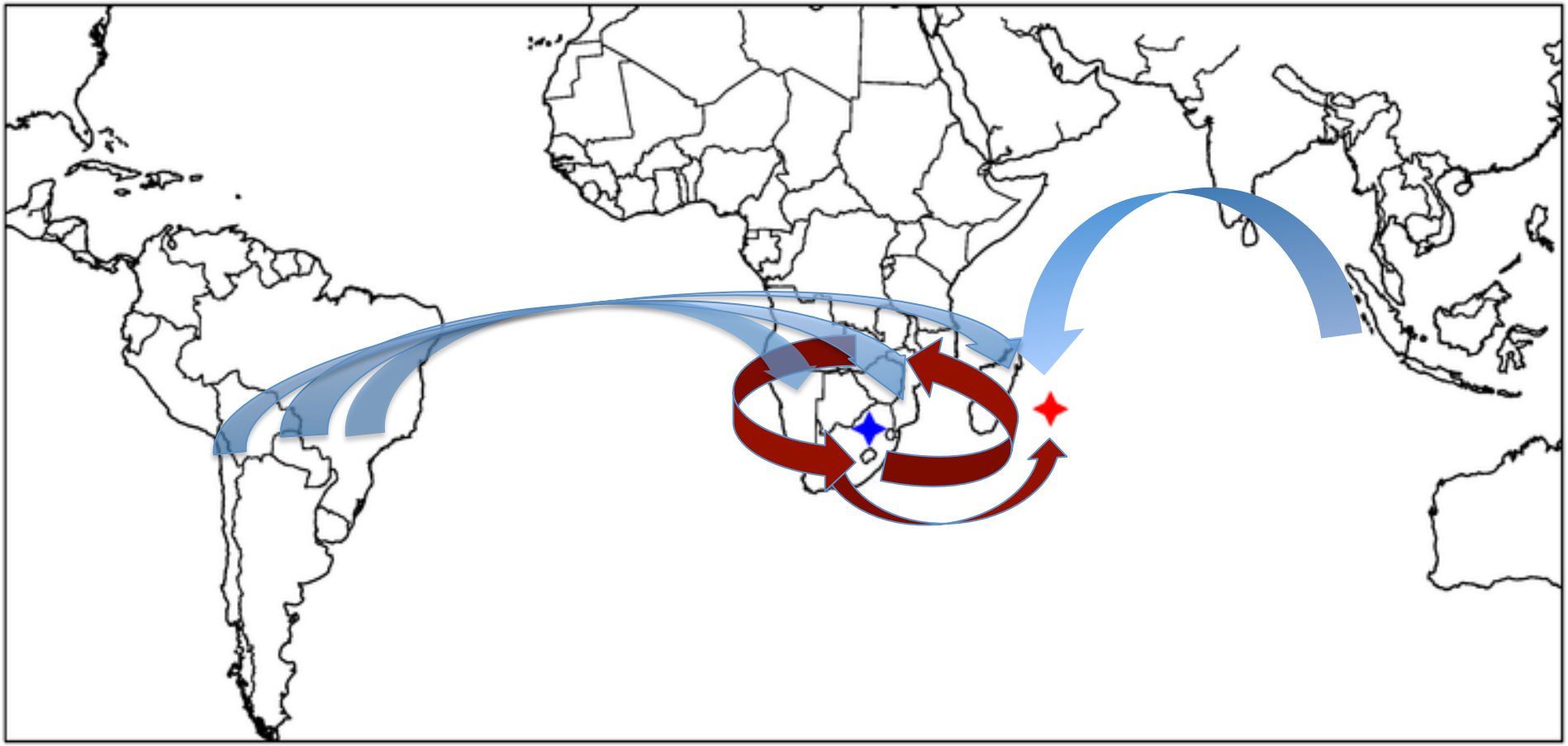

Figure 2

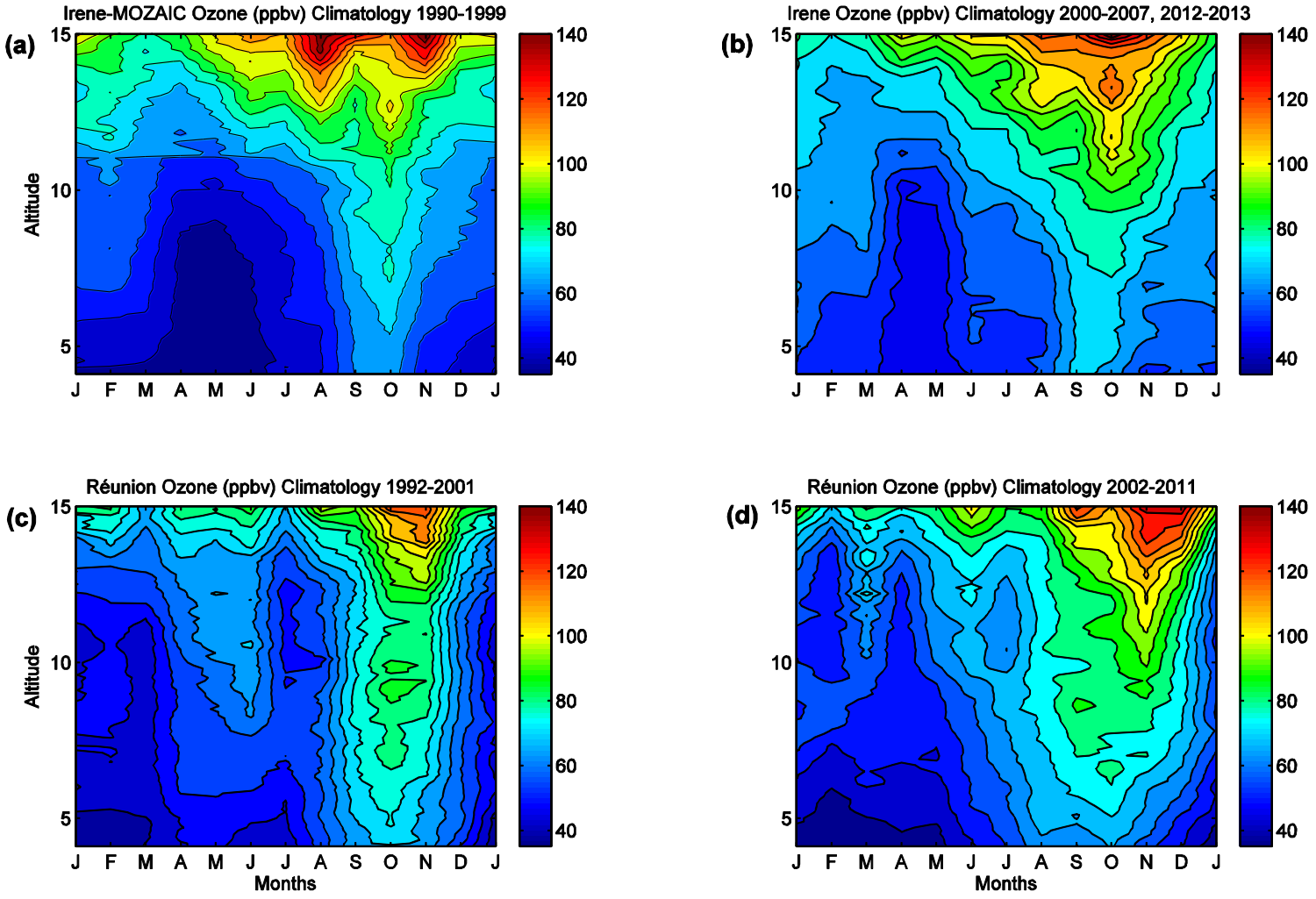
(a)
Irene-MOZAIC Ozone (ppbv) Climatology 1990-1999
(b)
Irene Ozone (ppbv) Climatology 2000-2007, 2012-2013
(c)
Réunion Ozone (ppbv) Climatology 1992-2001
(d)
Réunion Ozone (ppbv) Climatology 2002-2011
Altitude
15
10
5
J F M A M J J A S O N D J
Months
140
120
100
80
60
40

Figure 3

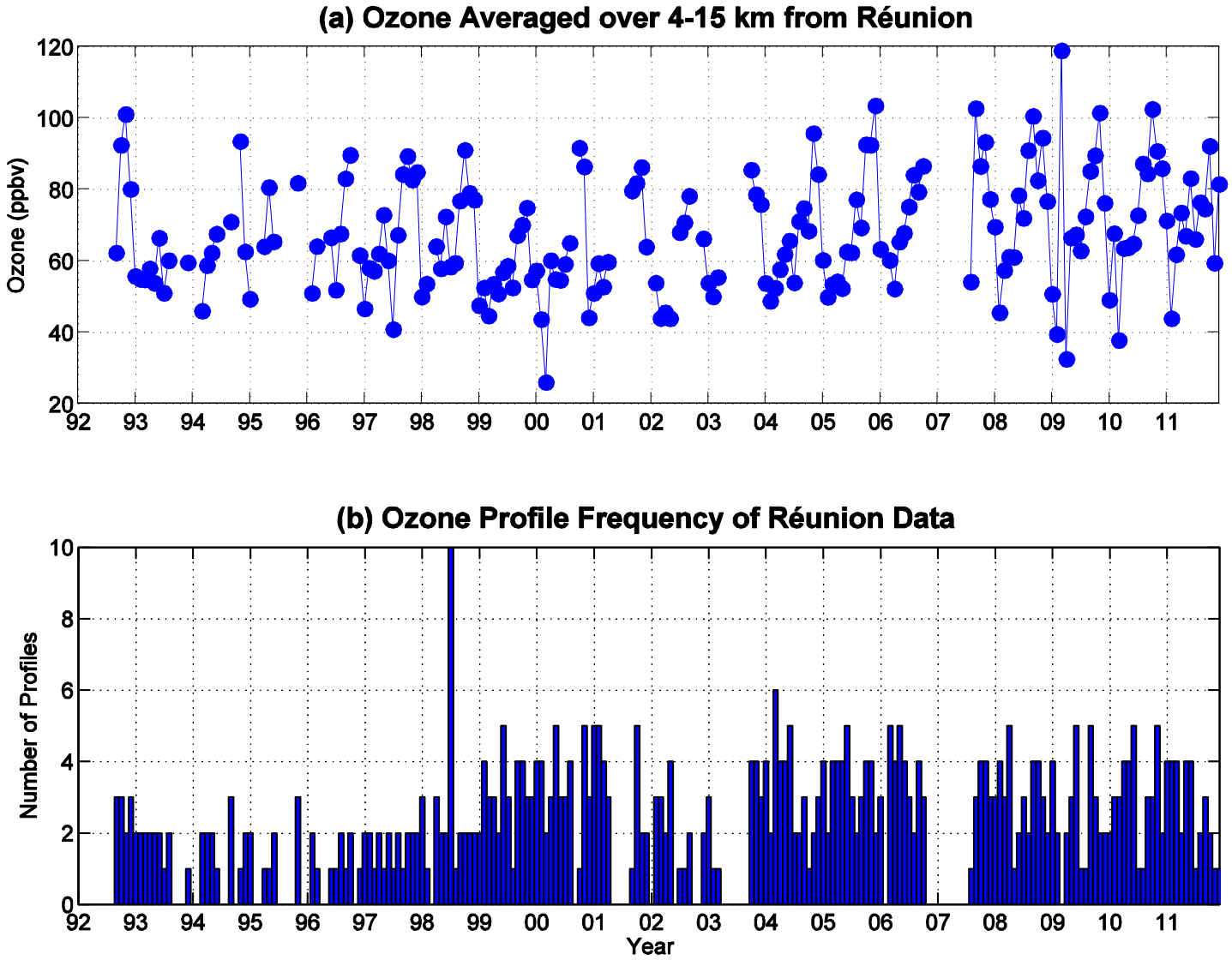
(a) Ozone Averaged over 4-15 km from Réunion
Ozone (ppbv)
120
100
80
60
40
20
92 93 94 95 96 97 98 99 00 01 02 03 04 05 06 07 08 09 10 11
(b) Ozone Profile Frequency of Réunion Data
Number of Profiles
10
8
6
4
2
0
92 93 94 95 96 97 98 99 00 01 02 03 04 05 06 07 08 09 10 11
Year

Figure 4

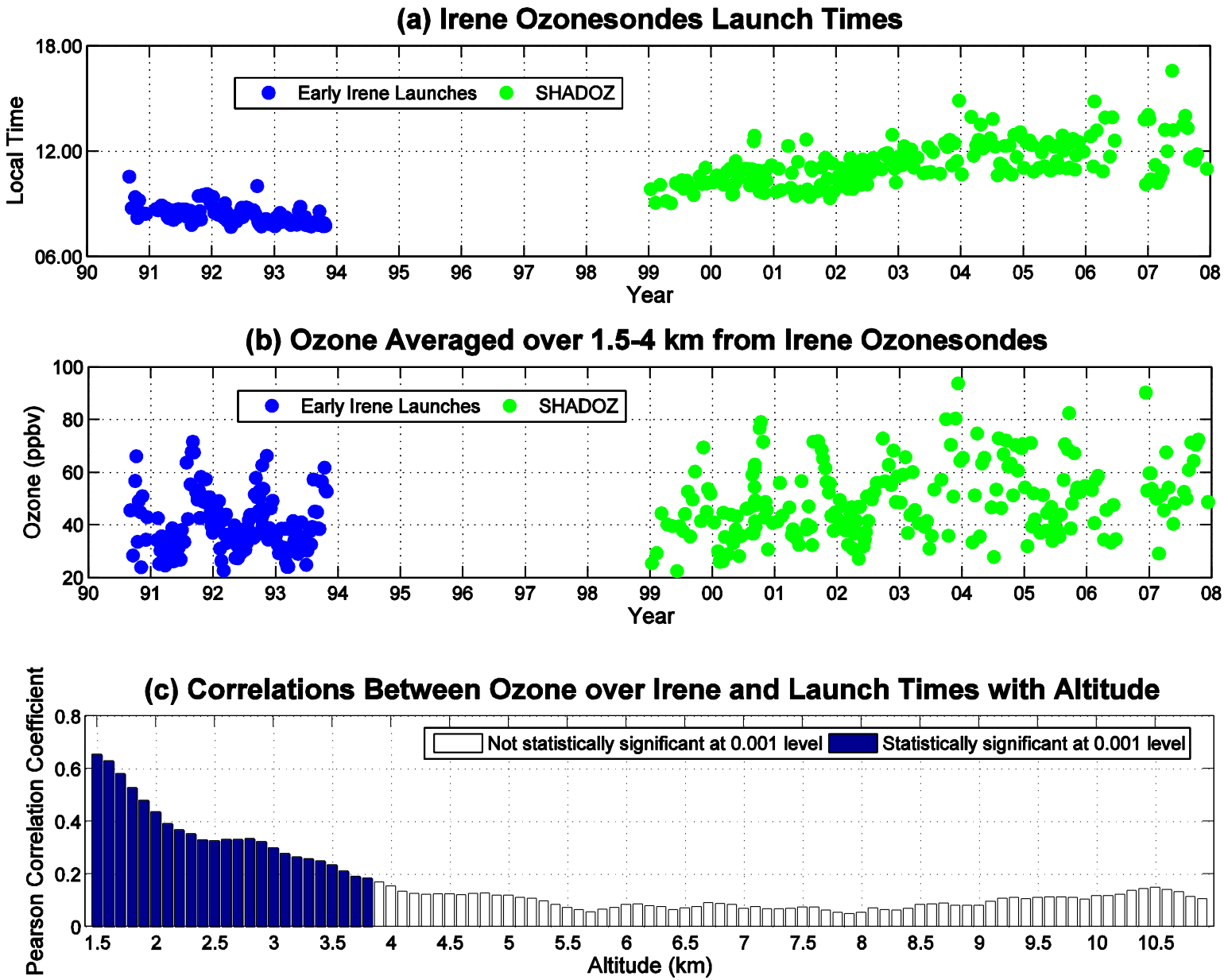
(a) Irene Ozonesondes Launch Times
Local Time
18.00
12.00
06.00
Early Irene Launches
SHADOZ
90 91 92 93 94 95 96 97 98 99 00 01 02 03 04 05 06 07 08
Year
(b) Ozone Averaged over 1.5-4 km from Irene Ozonesondes
Ozone (ppbv)
100
80
60
40
20
Early Irene Launches
SHADOZ
90 91 92 93 94 95 96 97 98 99 00 01 02 03 04 05 06 07 08
Year
(c) Correlations Between Ozone over Irene and Launch Times with Altitude
Pearson Correlation Coefficient
0.8
0.6
0.4
0.2
0
Not statistically significant at 0.001 level
Statistically significant at 0.001 level
1.5 2 2.5 3 3.5 4 4.5 5 5.5 6 6.5 7 7.5 8 8.5 9 9.5 10 10.5
Altitude (km)

Figure 5

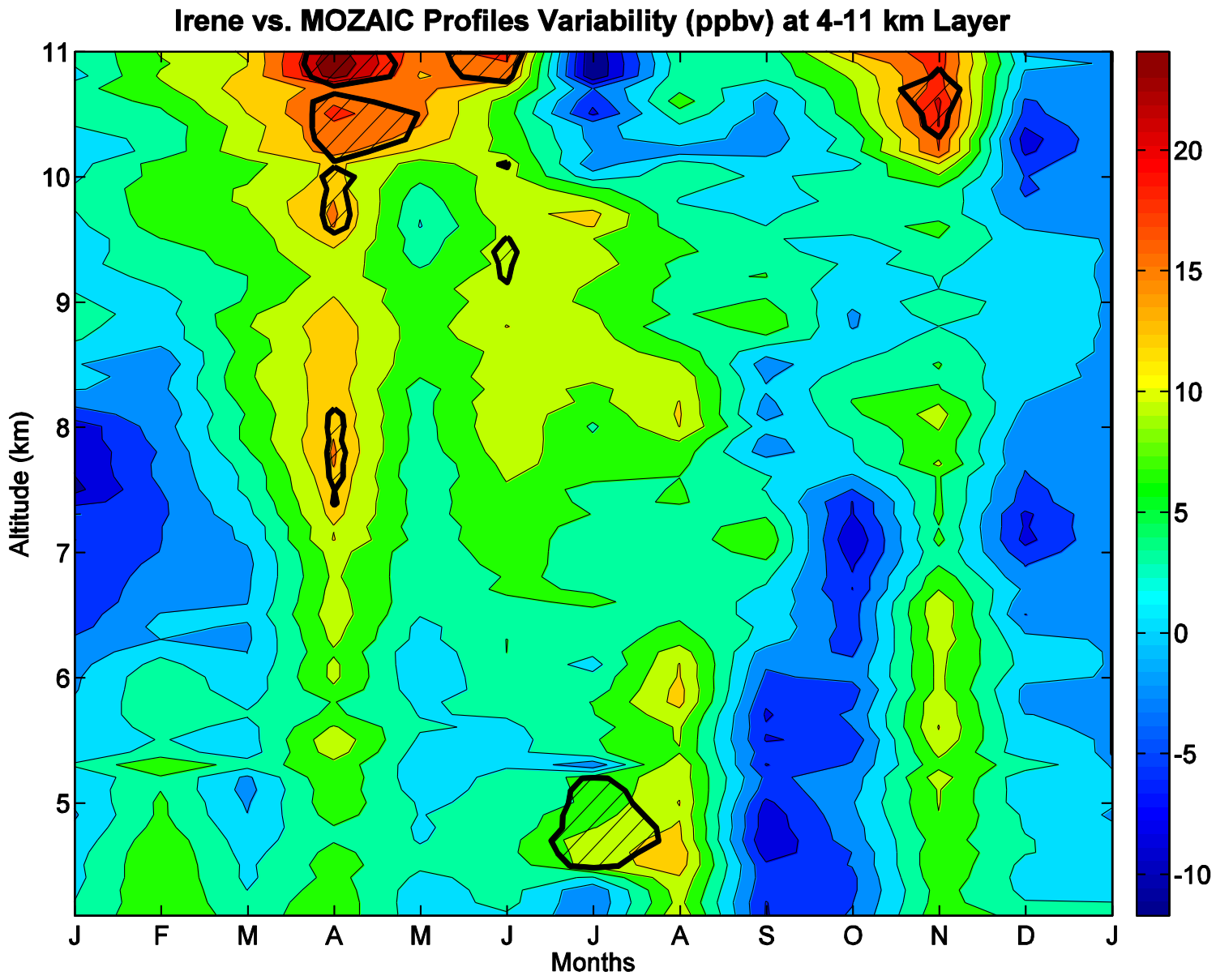
Irene vs. MOZAIC Profiles Variability (ppbv) at 4-11 km Layer
Altitude (km)
11
10
9
8
7
6
5
J
F
M
A
M
J
J
A
S
O
N
D
J
Months
20
15
10
5
0
-5
-10

Figure 6

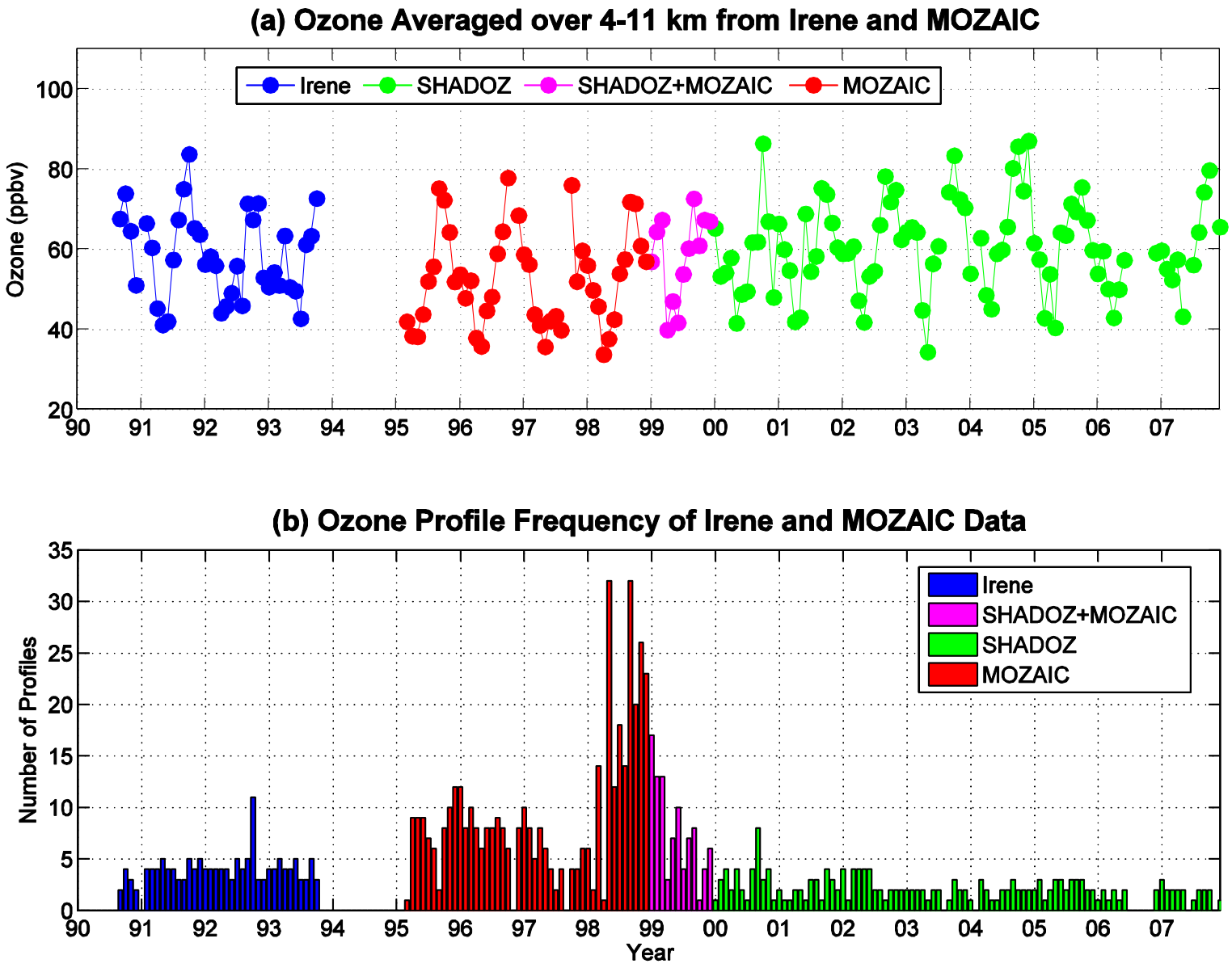
(a) Ozone Averaged over 4-11 km from Irene and MOZAIC
Irene
SHADOZ
SHADOZ+MOZAIC
MOZAIC
Ozone (ppbv)
20
40
60
80
100
90
91
92
93
94
95
96
97
98
99
00
01
02
03
04
05
06
07
(b) Ozone Profile Frequency of Irene and MOZAIC Data
Irene
SHADOZ+MOZAIC
SHADOZ
MOZAIC
Number of Profiles
0
5
10
15
20
25
30
35
Year

Figure 7

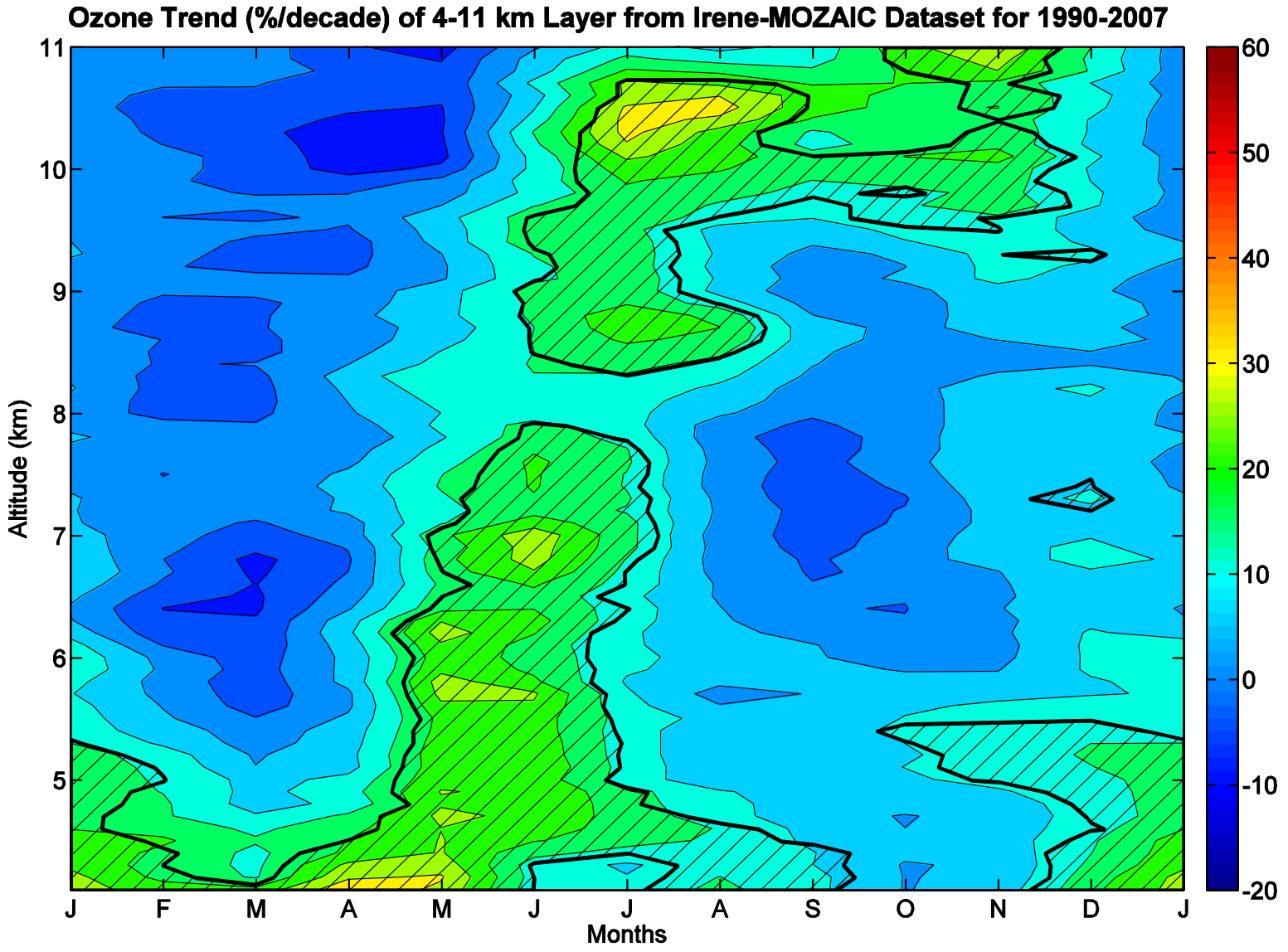
Ozone Trend (%/decade) of 4-11 km Layer from Irene-MOZAIC Dataset for 1990-2007
Altitude (km)
11
10
9
8
7
6
5
J
F
M
A
M
J
J
A
S
O
N
D
J
Months
60
50
40
30
20
10
0
-10
-20

Figure 8

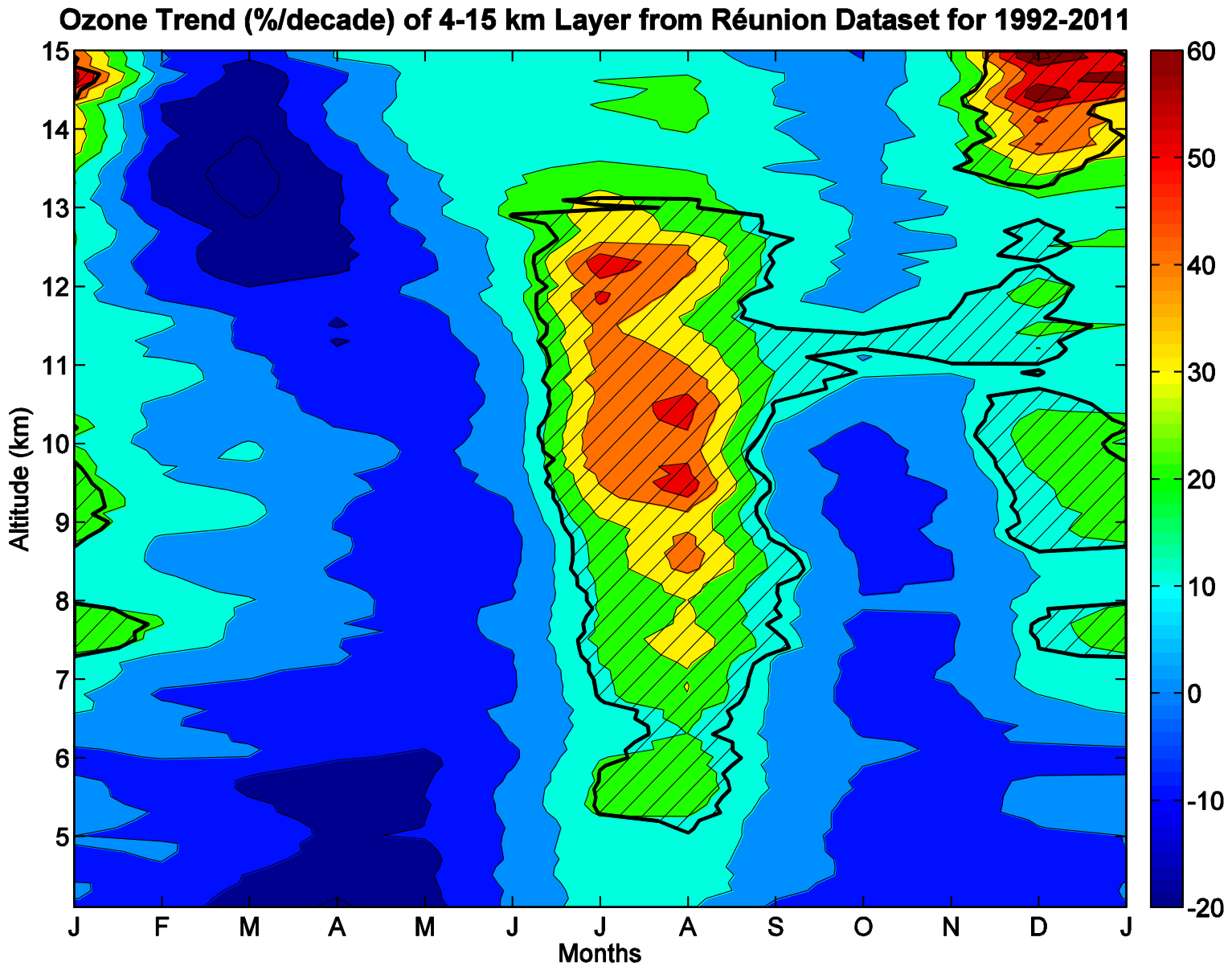
Ozone Trend (%/decade) of 4-15 km Layer from Réunion Dataset for 1992-2011
Altitude (km)
15
14
13
12
11
10
9
8
7
6
5
J
F
M
A
M
J
J
A
S
O
N
D
J
Months
60
50
40
30
20
10
0
-10
-20

Figure 9

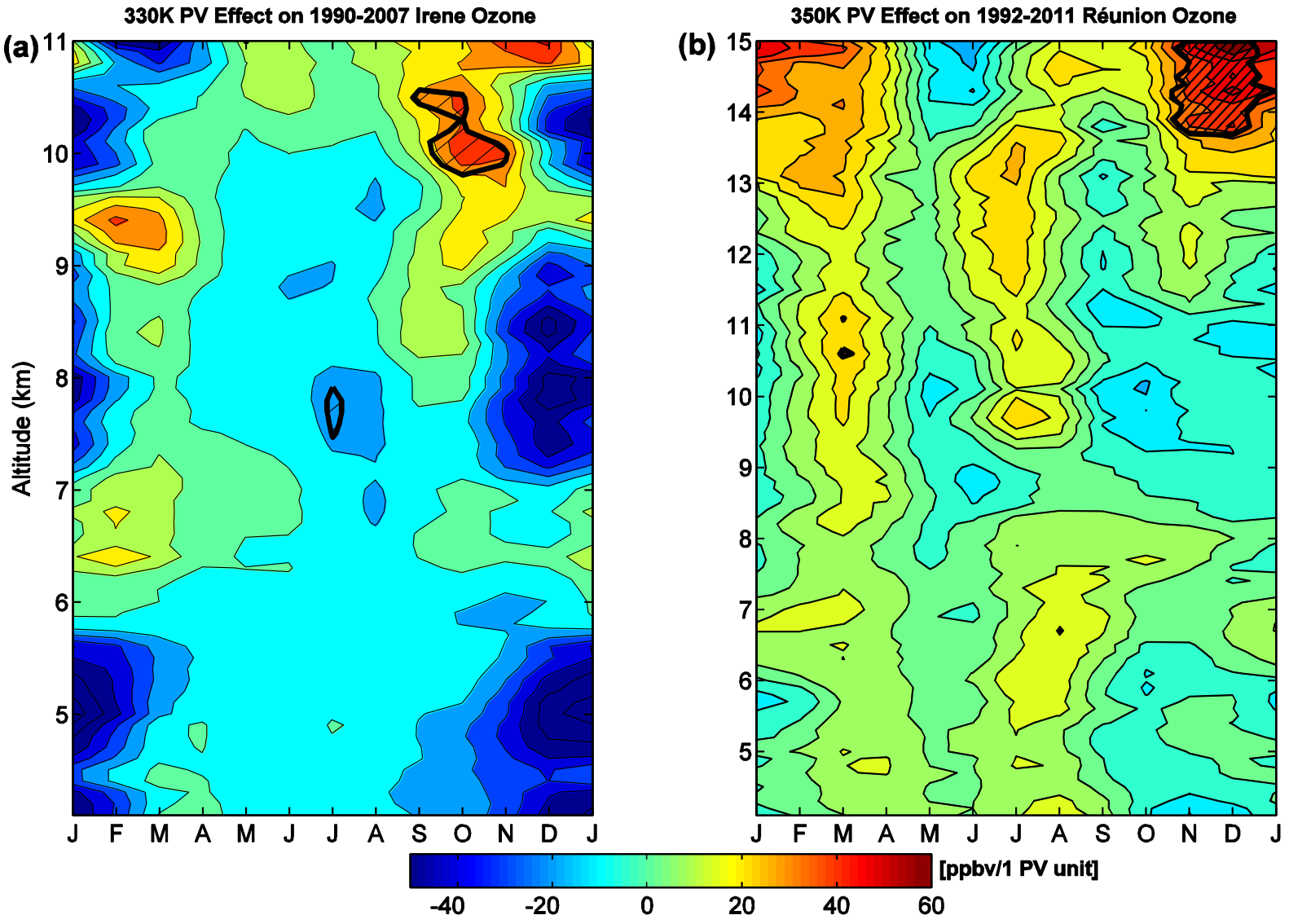
330K PV Effect on 1990-2007 Irene Ozone
(a)
Altitude (km)
11
10
9
8
7
6
5
J F M A M J J A S O N D J
350K PV Effect on 1992-2011 Réunion Ozone
(b)
15
14
13
12
11
10
9
8
7
6
5
J F M A M J J A S O N D J
[ppbv/1 PV unit]
-40 -20 0 20 40 60

Figure 10

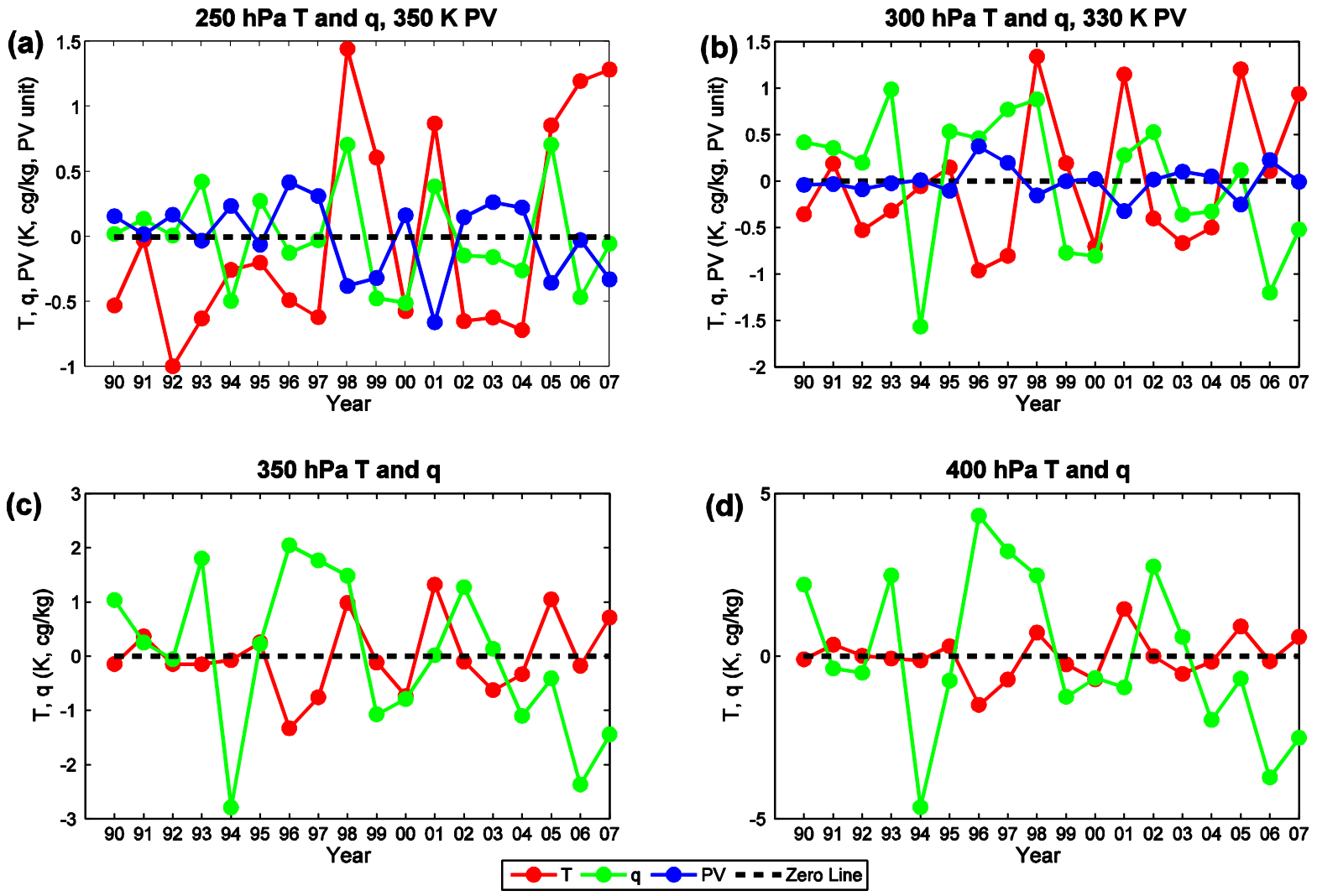
(a)
250 hPa T and q, 350 K PV
T, q, PV (K, cg/kg, PV unit)
Year
(b)
300 hPa T and q, 330 K PV
T, q, PV (K, cg/kg, PV unit)
Year
(c)
350 hPa T and q
T, q (K, cg/kg)
Year
(d)
400 hPa T and q
T, q (K, cg/kg)
Year
90 91 92 93 94 95 96 97 98 99 00 01 02 03 04 05 06 07
T
q
PV
Zero Line

Figure 11

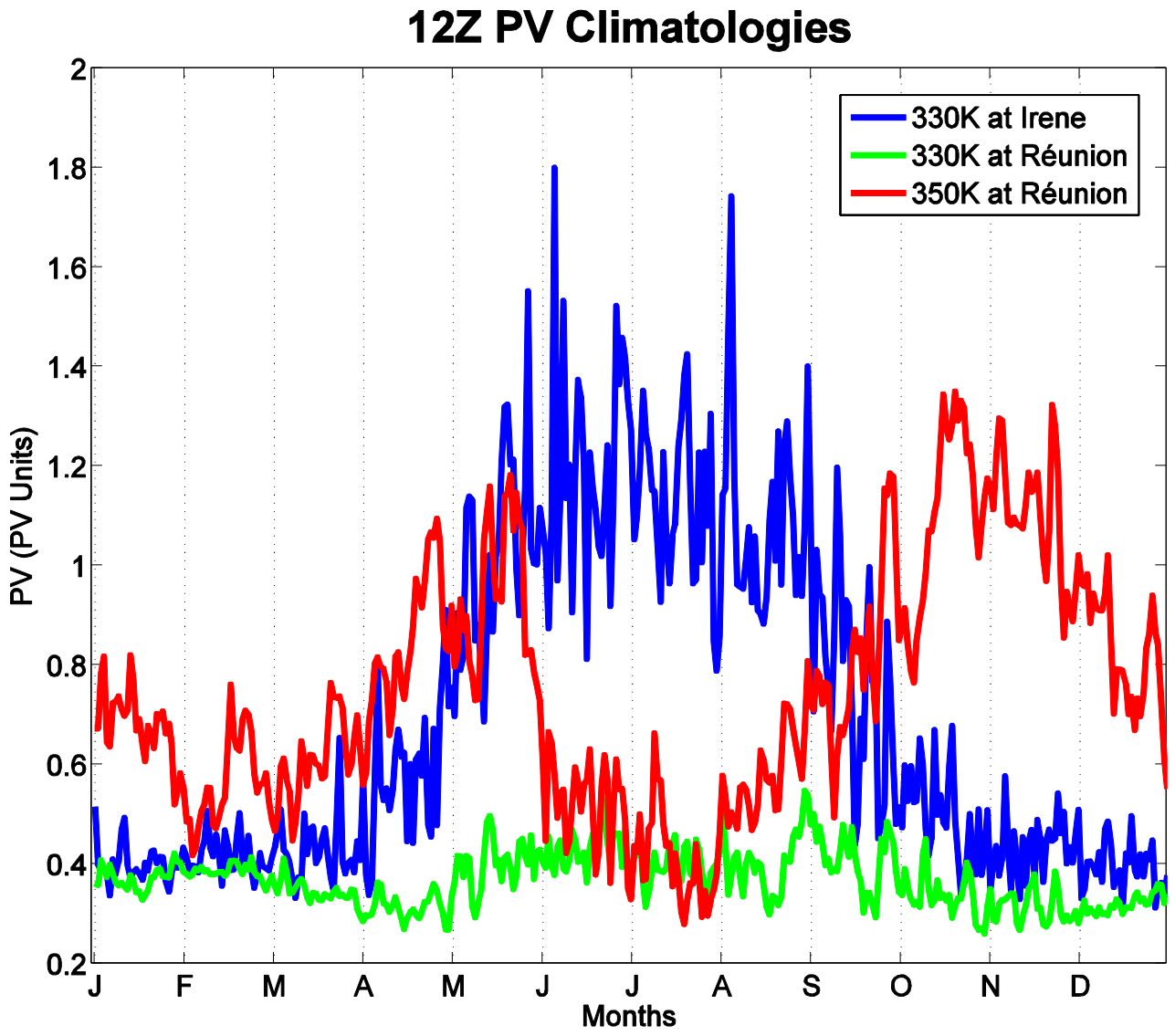
12Z PV Climatologies
330K at Irene
330K at Réunion
350K at Réunion
PV (PV Units)
2
1.8
1.6
1.4
1.2
1
0.8
0.6
0.4
0.2
J
F
M
A
M
J
J
A
S
O
N
D
Months

Figure 12

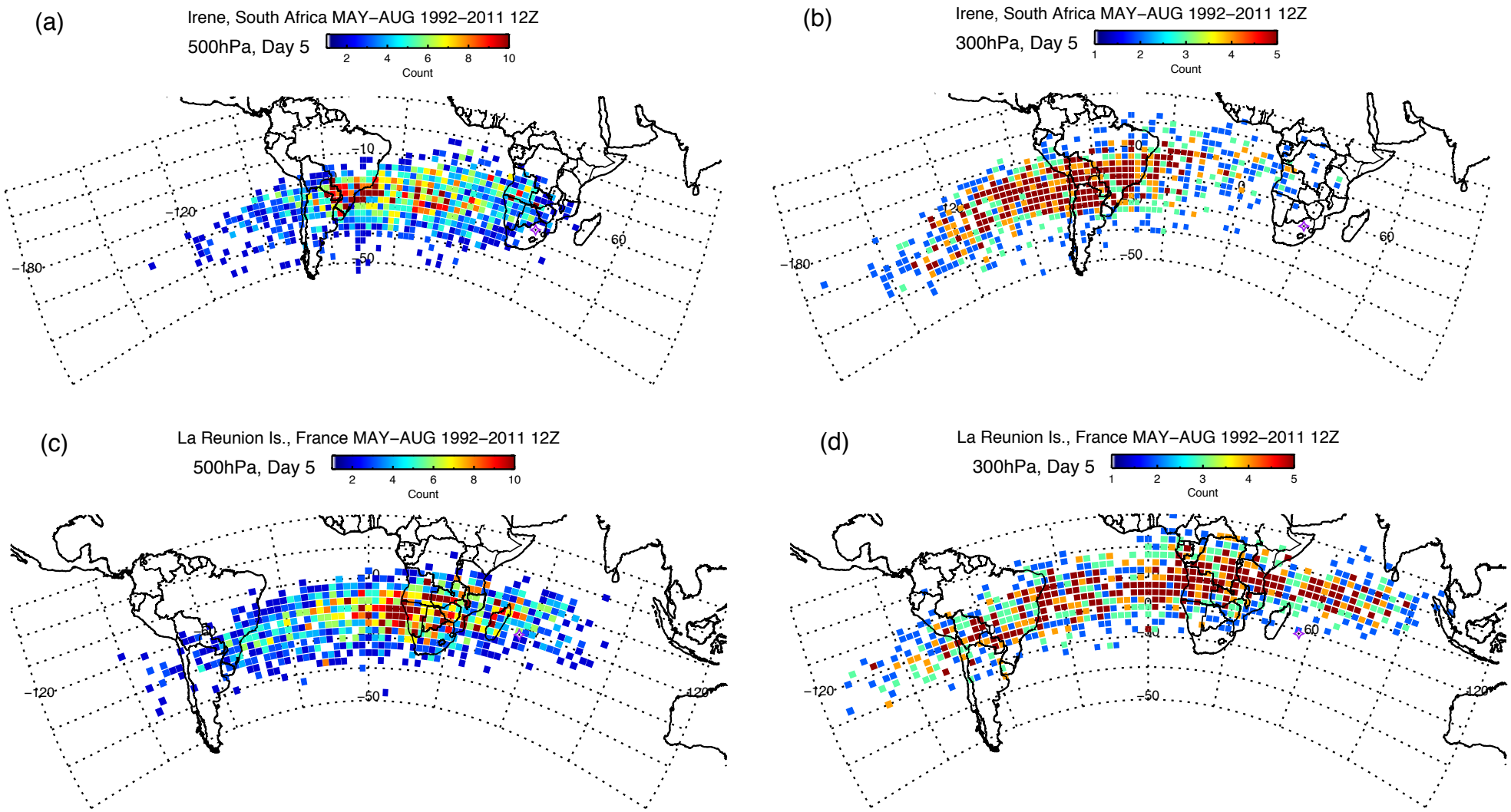
(a)
Irene, South Africa MAY–AUG 1992–2011 12Z
500hPa, Day 5
2 4 6 8 10
Count
(b)
Irene, South Africa MAY–AUG 1992–2011 12Z
300hPa, Day 5
1 2 3 4 5
Count
(c)
La Reunion Is., France MAY–AUG 1992–2011 12Z
500hPa, Day 5
2 4 6 8 10
Count
(d)
La Reunion Is., France MAY–AUG 1992–2011 12Z
300hPa, Day 5
1 2 3 4 5
Count

Figure 13

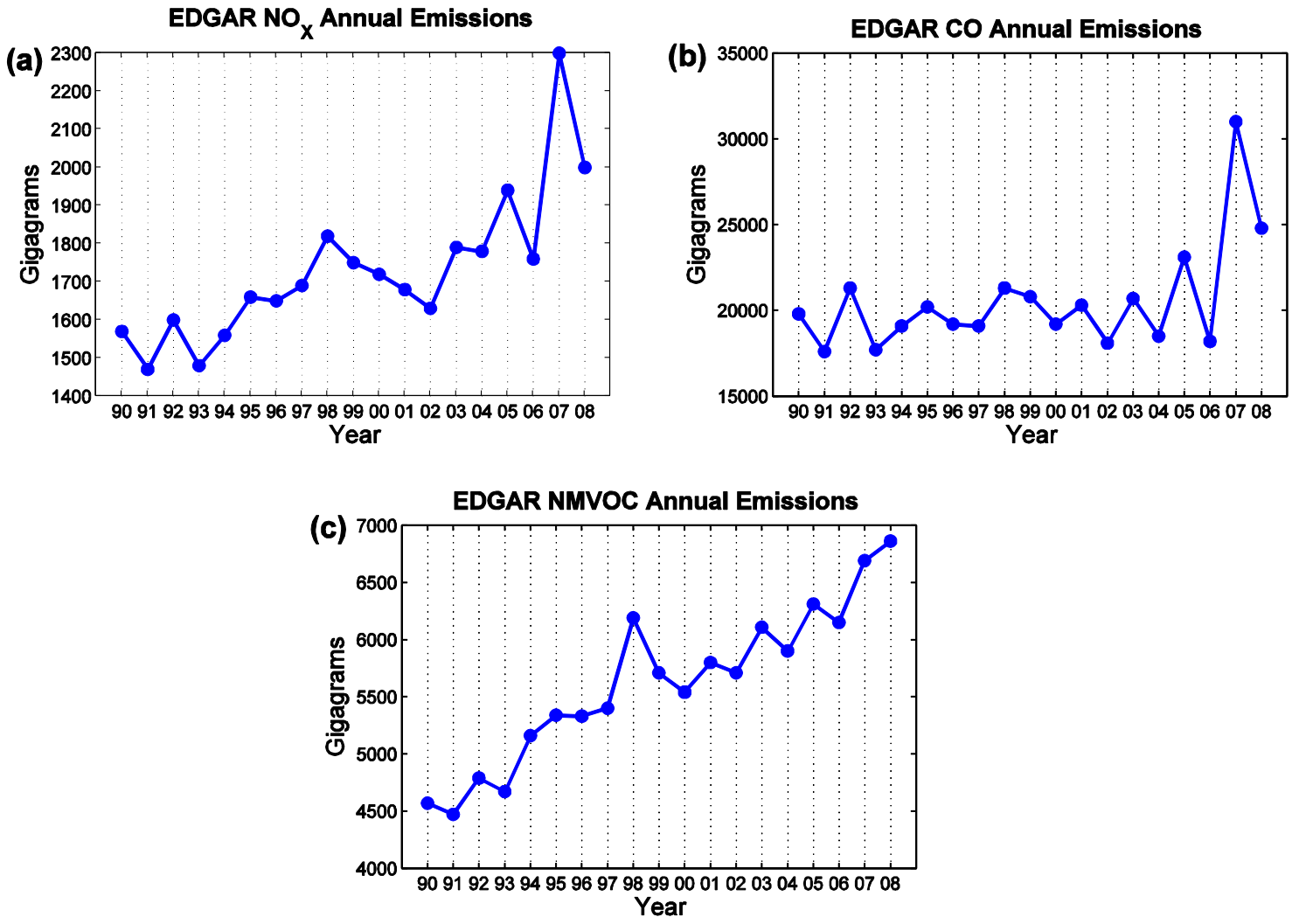
(a)
EDGAR NO$_X$ Annual Emissions
Gigagrams
2300
2200
2100
2000
1900
1800
1700
1600
1500
1400
90 91 92 93 94 95 96 97 98 99 00 01 02 03 04 05 06 07 08
Year
(b)
EDGAR CO Annual Emissions
Gigagrams
35000
30000
25000
20000
15000
90 91 92 93 94 95 96 97 98 99 00 01 02 03 04 05 06 07 08
Year
(c)
EDGAR NMVOC Annual Emissions
Gigagrams
7000
6500
6000
5500
5000
4500
4000
90 91 92 93 94 95 96 97 98 99 00 01 02 03 04 05 06 07 08
Year

Figure 14

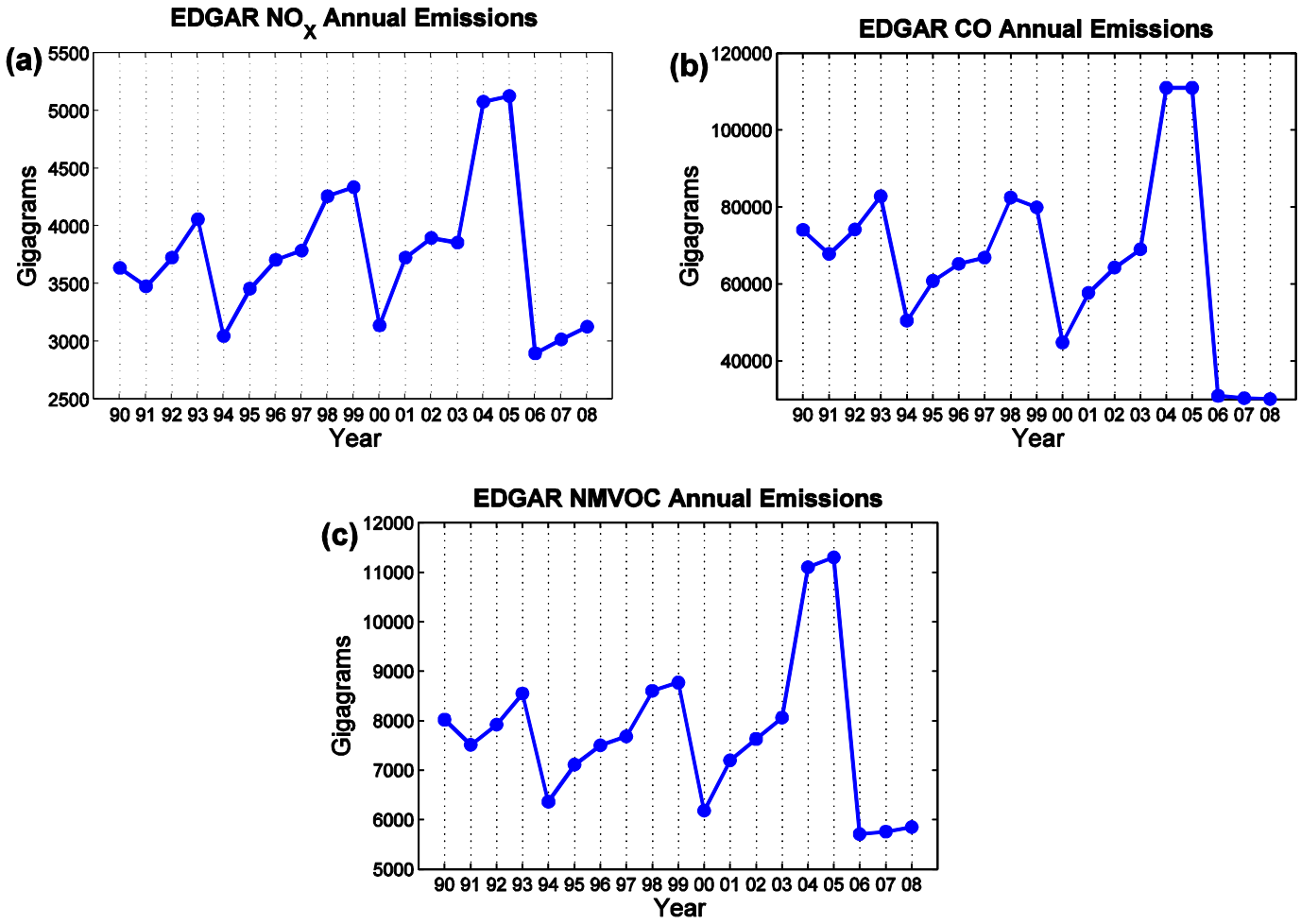
EDGAR NO_X Annual Emissions
(a)
Gigagrams
5500
5000
4500
4000
3500
3000
2500
90 91 92 93 94 95 96 97 98 99 00 01 02 03 04 05 06 07 08
Year
EDGAR CO Annual Emissions
(b)
Gigagrams
120000
100000
80000
60000
40000
90 91 92 93 94 95 96 97 98 99 00 01 02 03 04 05 06 07 08
Year
EDGAR NMVOC Annual Emissions
(c)
Gigagrams
12000
11000
10000
9000
8000
7000
6000
5000
90 91 92 93 94 95 96 97 98 99 00 01 02 03 04 05 06 07 08
Year